SUPPLEMENTAL MATERIAL

Nanoparticle Delivery of STAT3 Alleviates Pulmonary Hypertension in a Mouse Model of Alveolar Capillary Dysplasia

Fei Sun[1], Guolun Wang[1], Arun Pradhan[1], Kui Xu[1], Jose Gomez-Arroyo[1,2], Yufang Zhang[1], Gregory T. Kalin[1,3], Zicheng Deng[1,4], Ronald J Vagnozzi[5], Hua He[3], Andrew W. Dunn[1,4], Yuhua Wang[6], Allen J. York[5], Rashmi S. Hegde[6,7], Jason C Woods[7,8], Tanya V. Kalin[3,7], Jeffery D. Molkentin[5,7,9] and Vladimir V. Kalinichenko[1,3,6,7,*]

[1]Center for Lung Regenerative Medicine, Perinatal Institute, Cincinnati Children's Hospital Medical Center, Cincinnati, USA.
[2]Department of Internal Medicine, Section of Pulmonary and Critical Care, University of Cincinnati, Cincinnati, USA.
[3]Division of Pulmonary Biology, Cincinnati Children's Hospital Medical Center, Cincinnati, USA.
[4]The Materials Science and Engineering Program, College of Engineering and Applied Science, University of Cincinnati, Cincinnati, USA.
[5]Division of Molecular Cardiovascular Biology, Heart Institute, Cincinnati Children's Hospital Medical Center, Cincinnati, USA.
[6]Division of Developmental Biology, Cincinnati Children's Hospital Medical Center, Cincinnati, USA.
[7]Department of Pediatrics, University of Cincinnati, Cincinnati Children's Hospital Medical Center, Cincinnati, USA.
[8]Center for Pulmonary Imaging Research, Division of Pulmonary Medicine, Cincinnati Children's Hospital Medical Center, Cincinnati, USA.
[9]Howard Hughes Medical Institute, Cincinnati Children's Hospital Medical Center, Cincinnati, USA.

SUPPLEMENTAL TABLES

Supplemental Table I. Antibodies used for Immunofluorescence (IF), Western blot (WB) and Flow cytometry (FC).

Antibody	Assay	Company	Catalog No.
Endomucin	IF	Abcam	ab106100
αSMA	IF	Sigma	A5228
FOXF1	IF	RD systems	AF4798
PDGFRα	IF	RD systems	AF1062
p-STAT3	IF/WB	Cell signaling Technology	9145
STAT3	IF/WB	Santa Cruz	sc-7179
PECAM1	IF	RD Systems	553370
Ki-67	IF	Abcam	ab16667
VEGFA	IF	Santa Cruz	sc-152
HIF-1A	IF	Novus Biologicals	NB100-105
β-Actin	WB	Santa Cruz	sc-47778
CD45	FC	eBioscience	47-0451-82
CD326	FC	eBioscience	17-5791-82
CD31	FC	eBioscience	48-0311-82
CD140a	FC	eBioscience	25-1401-82
αSMA	FC	eBioscience	50-9760-80
Ki-67	FC	Biolegend	652428

Supplemental Table II. TaqMan primers used for qRT-PCR reactions.

Mouse TaqMan Gene expression assay	Catalog No.
Nppa	Mm01255747_g1
Nppb	Mm01255770_g1
Myh7	Mm00600555_m1
Myh6	Mm00440359_m1
Actb	Mm00607939_s1
Acta2	Mm00725412_s1
Pecam1	Mm01242584_m1
Flk1	Mm01222421_m1
Col1a1	Mm00801666_g1
Col3a1	Mm00802300_m1
Vimentin	Mm01333430_m1
Col1a2	Mm00483888_m1
Col5a2	Mm00483675_m1
Hif1a	Mm00468869_m1
Vegfa	Mm00437306_m1
H19	Mm01156721_g1
Binp3	Mm00833810_g1
Epas1	Mm01236112_m1
Slc2a1	Mm00441473_m1

A

B

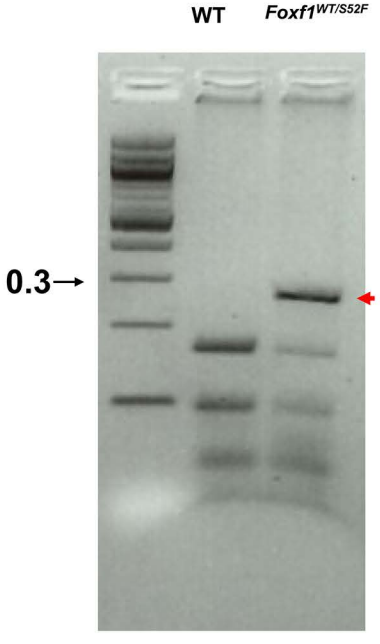

C

	WT	*Foxf1*$^{WT/S52F}$
RV area d apical (mm^2)	8.95 ± 0.58	12.11 ± 1.09*
RV area s apical (mm^2)	7.37 ± 0.46	9.73 ± 0.83*
RV area d SX (mm^2)	5.81 ± 0.51	7.98 ± 0.81*
RV area s SX (mm^2)	4.23 ± 0.37	6.23 ± 0.80*

D

	WT	*Foxf1*$^{WT/S52F}$
IVS;d (mm)	0.82 ± 0.04	0.78 ± 0.05
IVS;s (mm)	1.30 ± 0.06	1.11 ± 0.08
LA (mm)	2.14 ± 0.15	2.46 ± 0.15
LVID;d (mm)	4.00 ± 0.07	4.34 ± 0.10*
LVID;s (mm)	2.79 ± 0.13	3.12 ± 0.12
LVPW;d (mm)	0.71 ± 0.03	0.79 ± 0.04
LVPW;s (mm)	1.04 ± 0.05	1.13 ± 0.05
LV Mass (mg)	98.07 ± 6.26	93.93 ± 5.17
LV Vol;d (µl)	70.13 ± 3.01	85.11 ± 4.53*
LV Vol;s (µl)	30.26 ± 3.52	39.07 ± 3.51

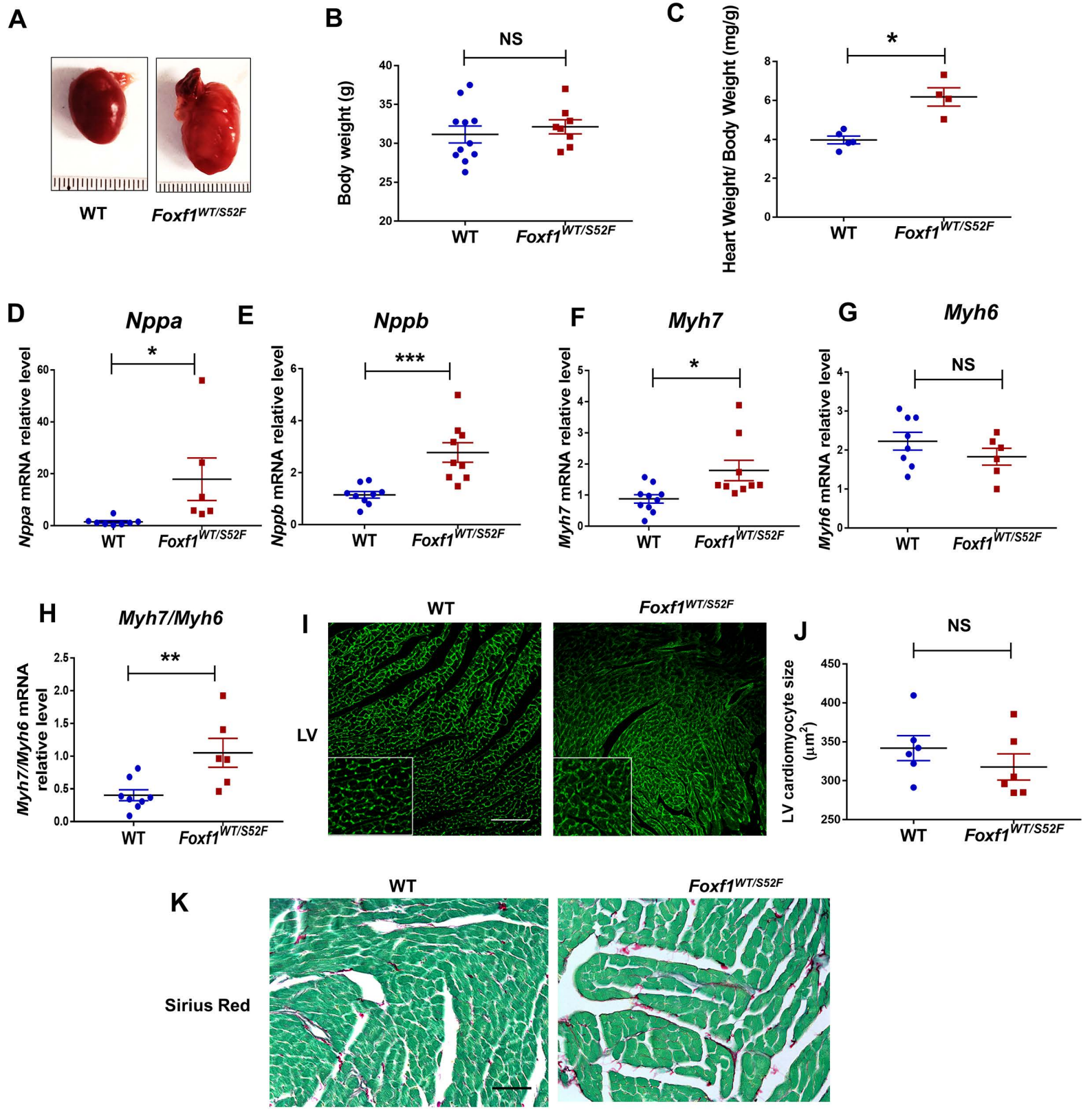
A
WT
Foxf1WT/S52F
B
NS
Body weight (g)
WT
Foxf1WT/S52F
C
*
Heart Weight/ Body Weight (mg/g)
WT
Foxf1WT/S52F
D
Nppa
*
Nppa mRNA relative level
WT
Foxf1WT/S52F
E
Nppb
***
Nppb mRNA relative level
WT
Foxf1WT/S52F
F
Myh7
*
Myh7 mRNA relative level
WT
Foxf1WT/S52F
G
Myh6
NS
Myh6 mRNA relative level
WT
Foxf1WT/S52F
H
Myh7/Myh6
**
Myh7/Myh6 mRNA relative level
WT
Foxf1WT/S52F
I
WT
Foxf1WT/S52F
LV
J
NS
LV cardiomyocyte size (μm2)
WT
Foxf1WT/S52F
K
WT
Foxf1WT/S52F
Sirius Red

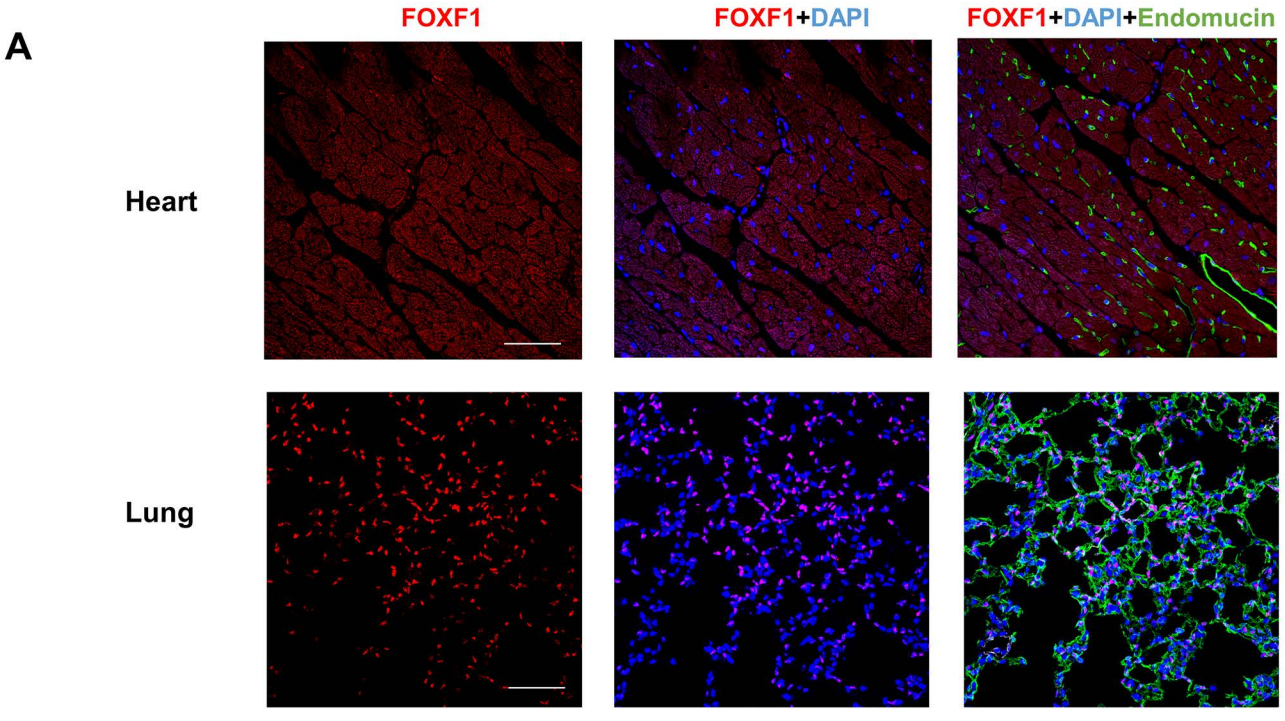

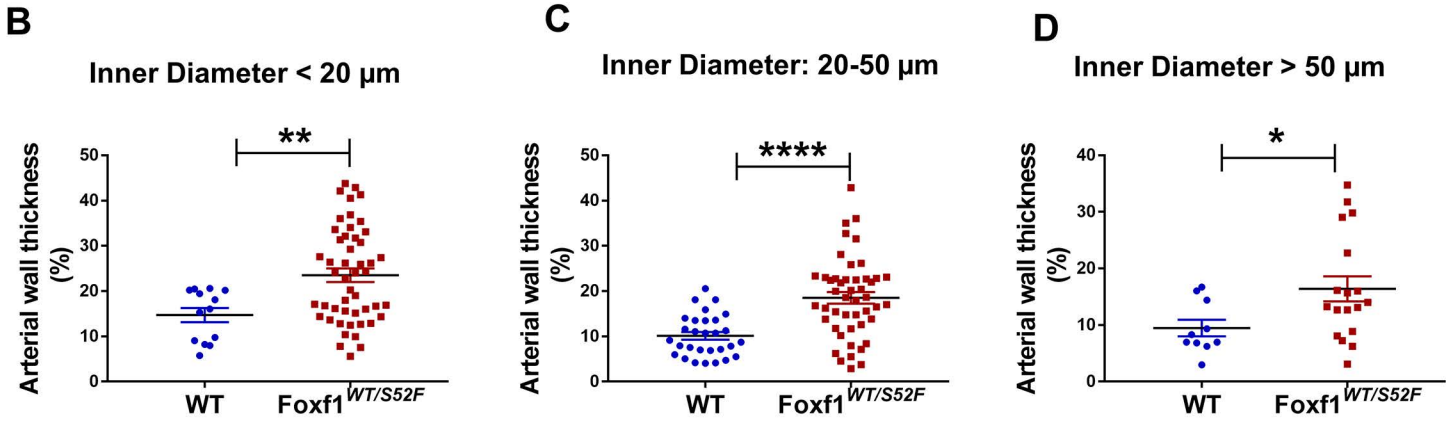

E

Mouse Genotype	WT			*Foxf1*$^{WT/S52F}$		
Arterial inner diameter (μm)	<20	20-50	>50	<20	20-50	>50
% of non-remodeled	0.00%	0.00%	0.00%	46.94%	61.70%	72.22%
% of partially remodeled	0.00%	0.00%	0.00%	53.06%	38.30%	27.78%
% of fully remodeled	0.00%	0.00%	0.00%	0.00%	0.00%	0.00%

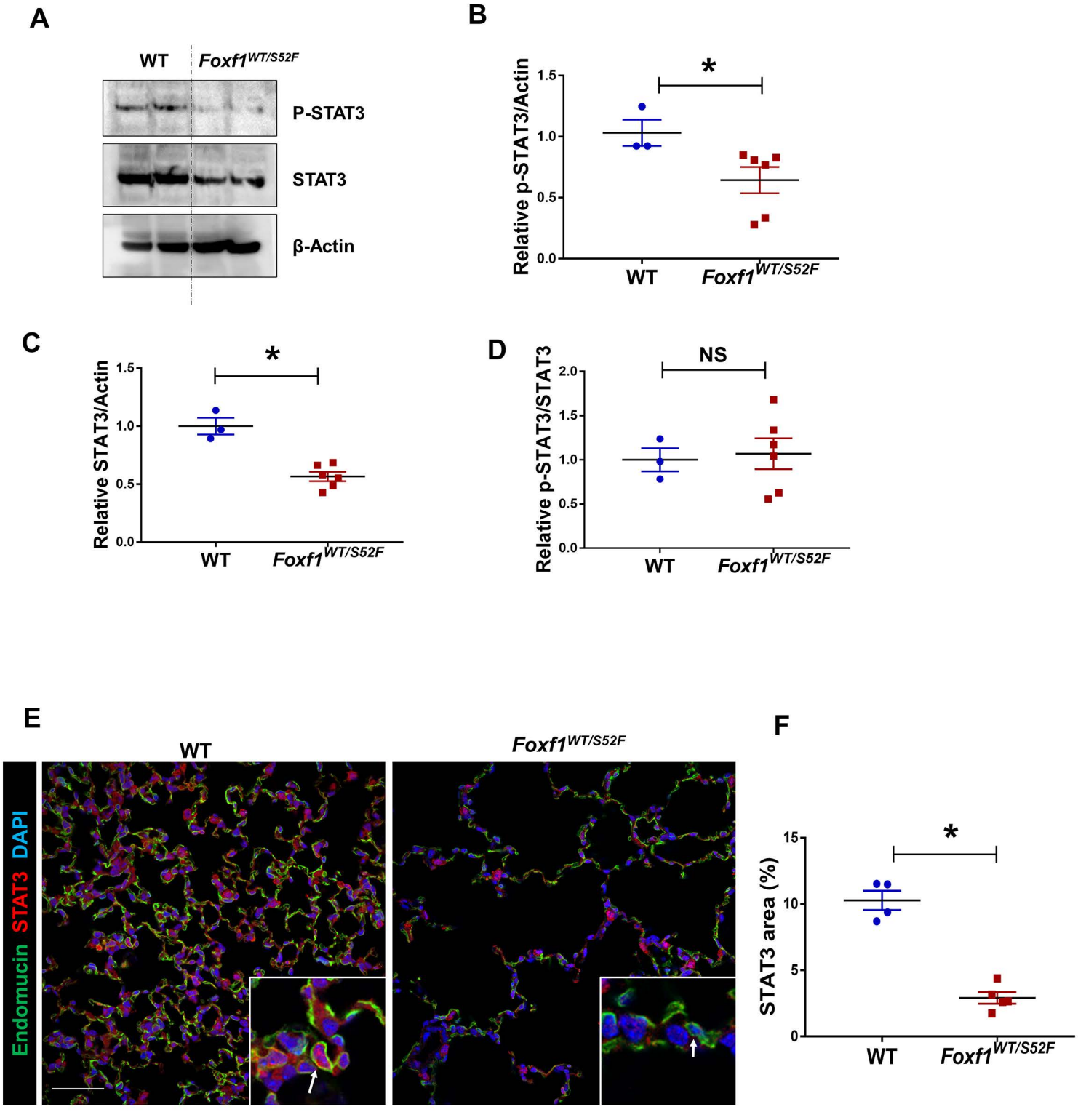
A
WT
Foxf1WT/S52F
P-STAT3
STAT3
β-Actin
B
Relative p-STAT3/Actin
1.5
1.0
0.5
0.0
*
WT
Foxf1WT/S52F
C
Relative STAT3/Actin
1.5
1.0
0.5
0.0
*
WT
Foxf1WT/S52F
D
Relative p-STAT3/STAT3
2.0
1.5
1.0
0.5
0.0
NS
WT
Foxf1WT/S52F
E
WT
Foxf1WT/S52F
Endomucin STAT3 DAPI
F
STAT3 area (%)
15
10
5
0
*
WT
Foxf1WT/S52F

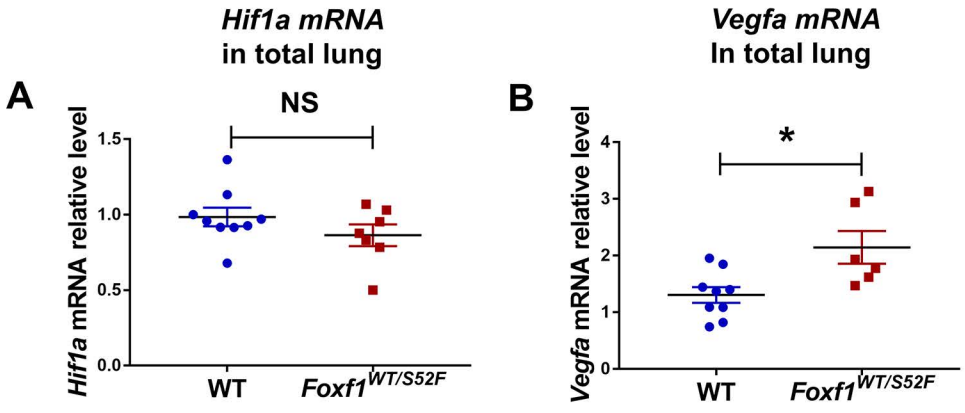
A
Hif1a mRNA
in total lung
NS
Hif1a mRNA relative level
1.5
1.0
0.5
0.0
WT
Foxf1WT/S52F
B
Vegfa mRNA
In total lung
*
Vegfa mRNA relative level
4
3
2
1
0
WT
Foxf1WT/S52F

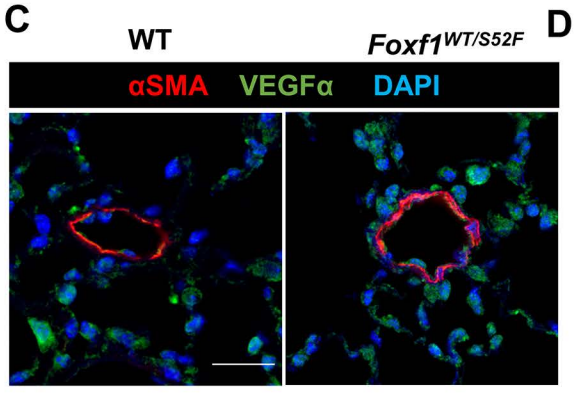
C
WT
Foxf1WT/S52F
αSMA
VEGFα
DAPI

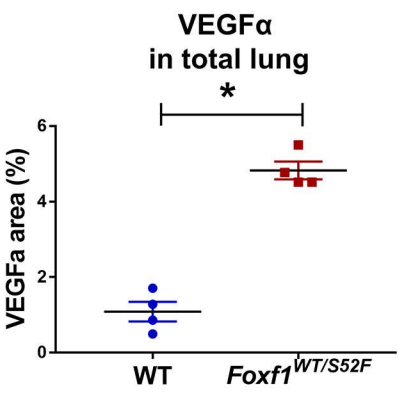
D
VEGFα
in total lung
*
VEGFa area (%)
6
4
2
0
WT
Foxf1WT/S52F

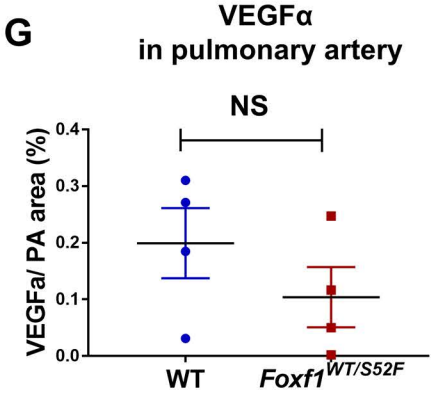
G
VEGFα
in pulmonary artery
NS
VEGFa/ PA area (%)
0.4
0.3
0.2
0.1
0.0
WT
Foxf1WT/S52F

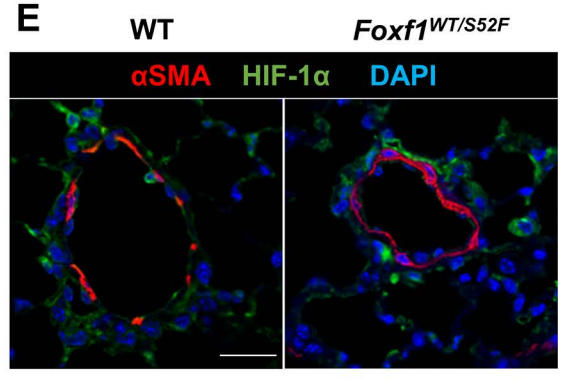
E
WT
Foxf1WT/S52F
αSMA
HIF-1α
DAPI

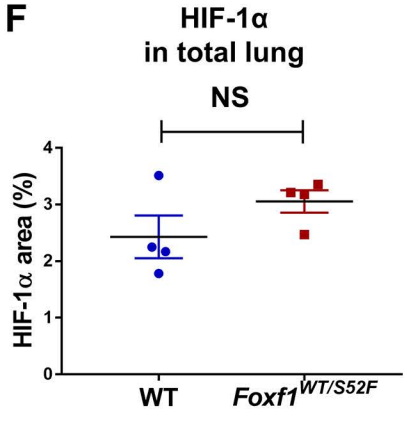
F
HIF-1α
in total lung
NS
HIF-1α area (%)
4
3
2
1
0
WT
Foxf1WT/S52F

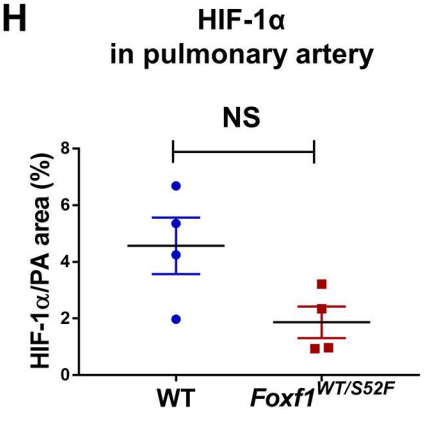
H
HIF-1α
in pulmonary artery
NS
HIF-1α/PA area (%)
8
6
4
2
0
WT
Foxf1WT/S52F

E17.5

A

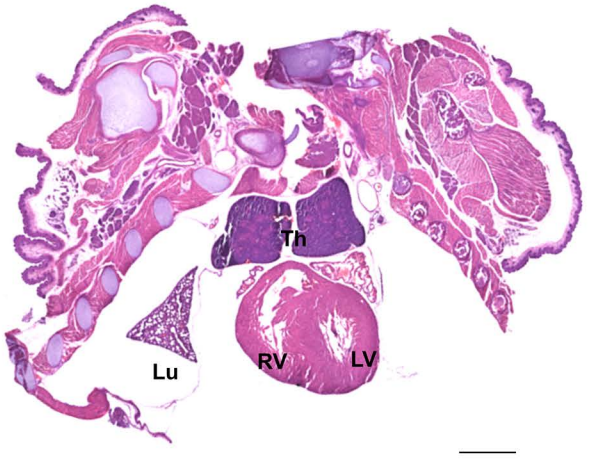

WT

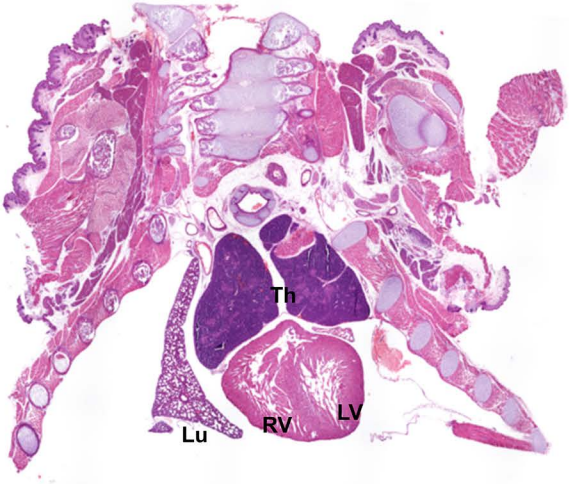

Foxf1$^{WT/S52F}$

B

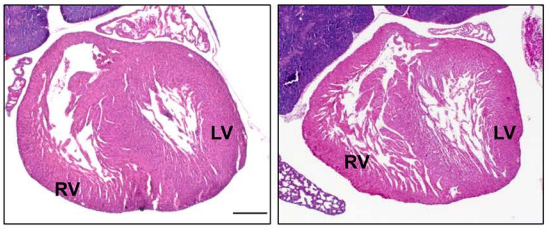

WT

Foxf1$^{WT/S52F}$

A

	WT				*Foxf1*$^{WT/S52F}$			
	Body weight (g)	Number of alive mice/ total mice	Number of dead mice during time period / total number of dead mice	Mortality (%)	Body weight (g)	Number of alive mice/ total mice	Number of dead mice during time period / total number of dead mice	Mortality (%)
P0	1.38 ± 0.02	32 / 32	0 / 0	0.00%	1.20 ± 0.46	8 / 13	5 / 5	38.46%
P7	4.78 ± 0.70	32 / 32	0 / 0	0.00%	2.79 ± 0.34	7 / 13	1 / 6	46.15%
P14	7.18 ± 0.14	32 / 32	0 / 0	0.00%	5.23 ± 0.60	6 / 13	1 / 7	53.84%
P21	8.50 ± 0.20	32 / 32	0 / 0	0.00%	7.20 ± 1.18	6 / 13	0 / 7	53.84%
P28	12.93 ± 0.31	32 / 32	0 / 0	0.00%	7.32 ± 1.16	4 / 13	2 / 9	69.23%

B

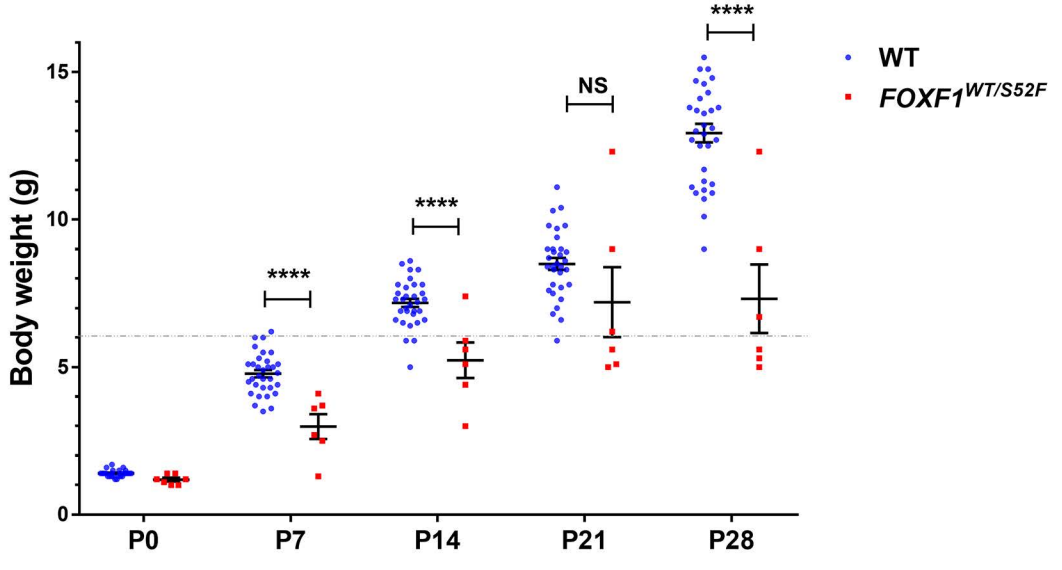

C

D

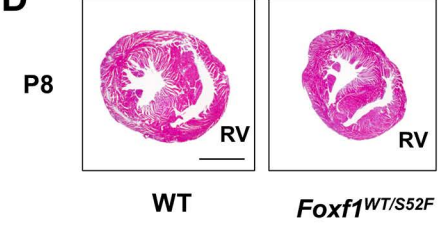

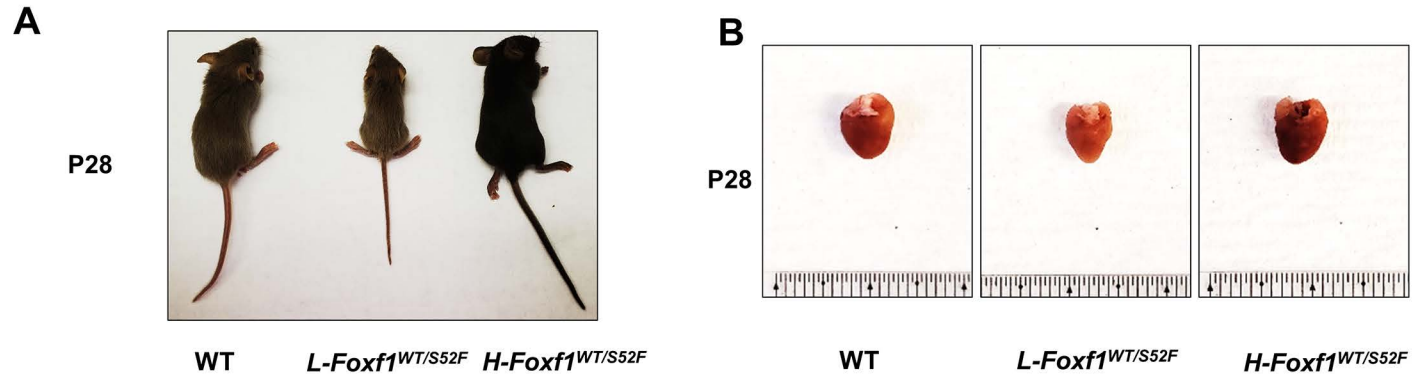
A
P28
WT
L-Foxf1WT/S52F
H-Foxf1WT/S52F
B
P28
WT
L-Foxf1WT/S52F
H-Foxf1WT/S52F

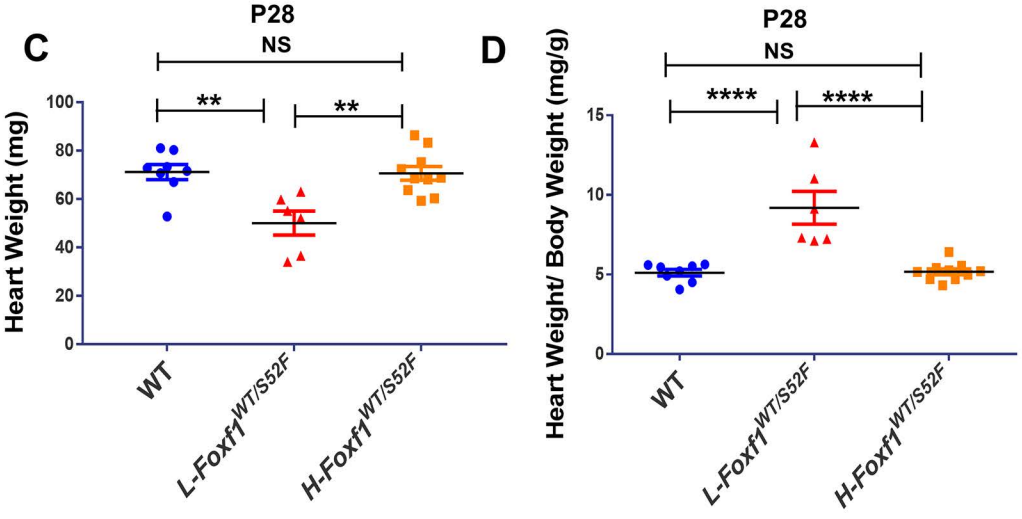
C
P28
NS
**
**
Heart Weight (mg)
100
80
60
40
20
0
WT
L-Foxf1WT/S52F
H-Foxf1WT/S52F
D
P28
NS
****
****
Heart Weight/ Body Weight (mg/g)
15
10
5
0
WT
L-Foxf1WT/S52F
H-Foxf1WT/S52F

Fei et al., Suppl.Fig.IX

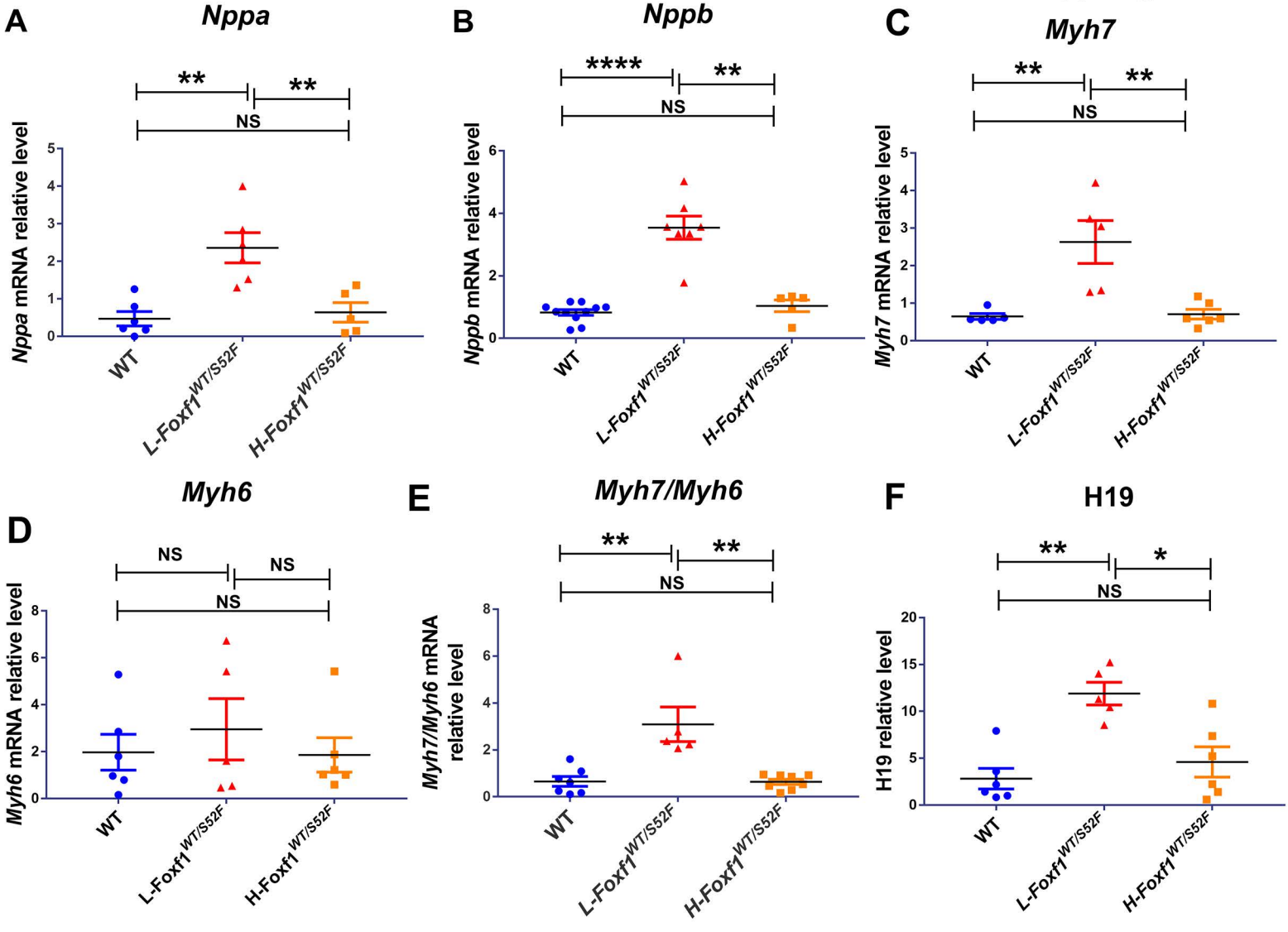

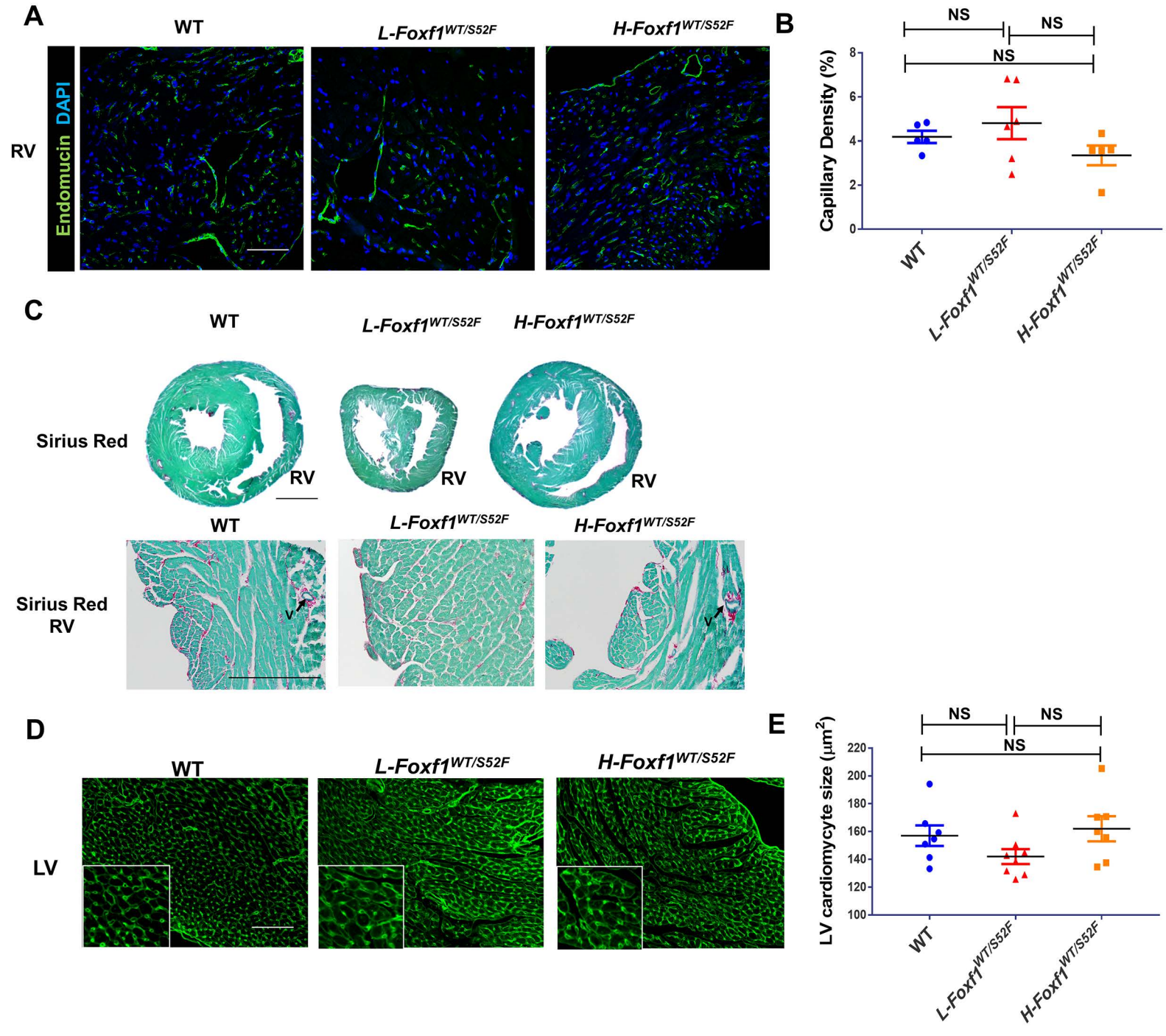
A
WT
L-Foxf1WT/S52F
H-Foxf1WT/S52F
RV
Endomucin DAPI
B
NS
NS
NS
Capillary Density (%)
0
2
4
6
8
WT
L-Foxf1WT/S52F
H-Foxf1WT/S52F
C
WT
L-Foxf1WT/S52F
H-Foxf1WT/S52F
Sirius Red
RV
RV
RV
Sirius Red RV
WT
L-Foxf1WT/S52F
H-Foxf1WT/S52F
V
V
D
WT
L-Foxf1WT/S52F
H-Foxf1WT/S52F
LV
E
NS
NS
NS
LV cardiomycyte size (μm2)
100
120
140
160
180
200
220
WT
L-Foxf1WT/S52F
H-Foxf1WT/S52F

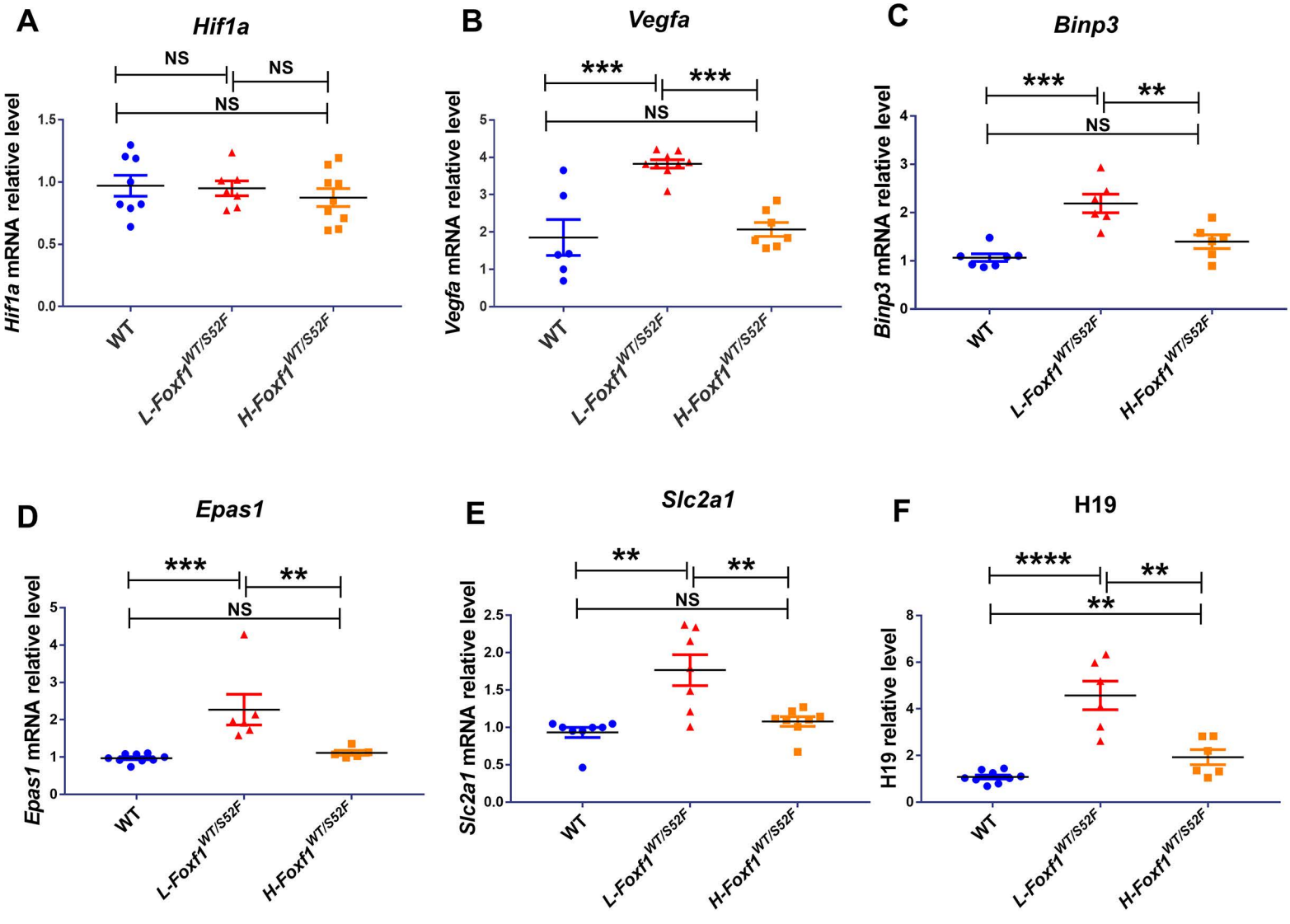
A
Hif1a
Hif1a mRNA relative level
NS
NS
NS
1.5
1.0
0.5
0.0
WT
L-Foxf1WT/S52F
H-Foxf1WT/S52F
B
Vegfa
Vegfa mRNA relative level
***
***
NS
5
4
3
2
1
0
WT
L-Foxf1WT/S52F
H-Foxf1WT/S52F
C
Binp3
Binp3 mRNA relative level
***
**
NS
4
3
2
1
0
WT
L-Foxf1WT/S52F
H-Foxf1WT/S52F
D
Epas1
Epas1 mRNA relative level
***
**
NS
5
4
3
2
1
0
WT
L-Foxf1WT/S52F
H-Foxf1WT/S52F
E
Slc2a1
Slc2a1 mRNA relative level
**
**
NS
2.5
2.0
1.5
1.0
0.5
0.0
WT
L-Foxf1WT/S52F
H-Foxf1WT/S52F
F
H19
H19 relative level
****
**
**
8
6
4
2
0
WT
L-Foxf1WT/S52F
H-Foxf1WT/S52F

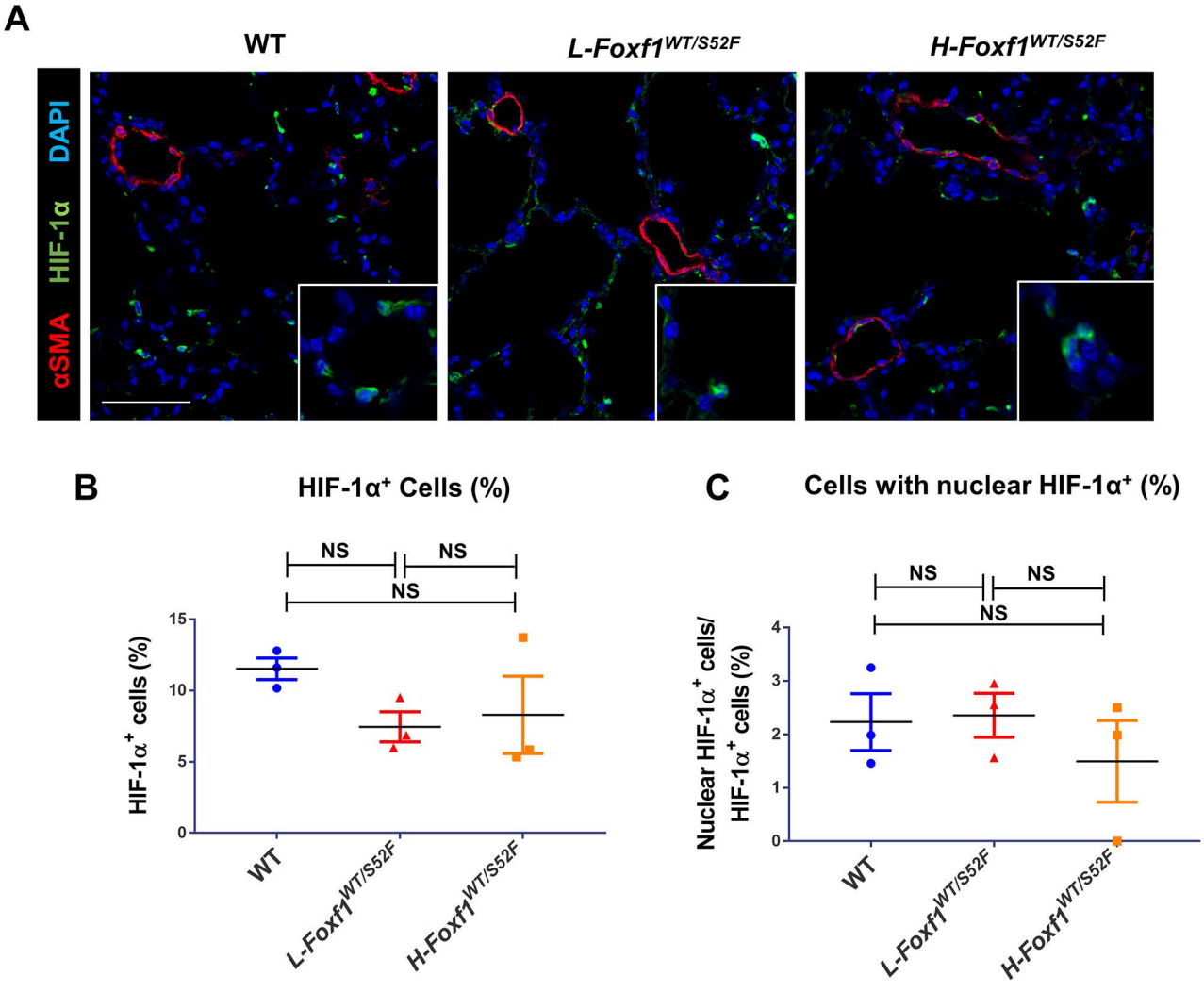
A
WT
L-Foxf1WT/S52F
H-Foxf1WT/S52F
αSMA
HIF-1α
DAPI
B
HIF-1α+ Cells (%)
NS
NS
NS
HIF-1α+ cells (%)
15
10
5
0
WT
L-Foxf1WT/S52F
H-Foxf1WT/S52F
C
Cells with nuclear HIF-1α+ (%)
NS
NS
NS
Nuclear HIF-1α+ cells/ HIF-1α+ cells (%)
4
3
2
1
0
WT
L-Foxf1WT/S52F
H-Foxf1WT/S52F

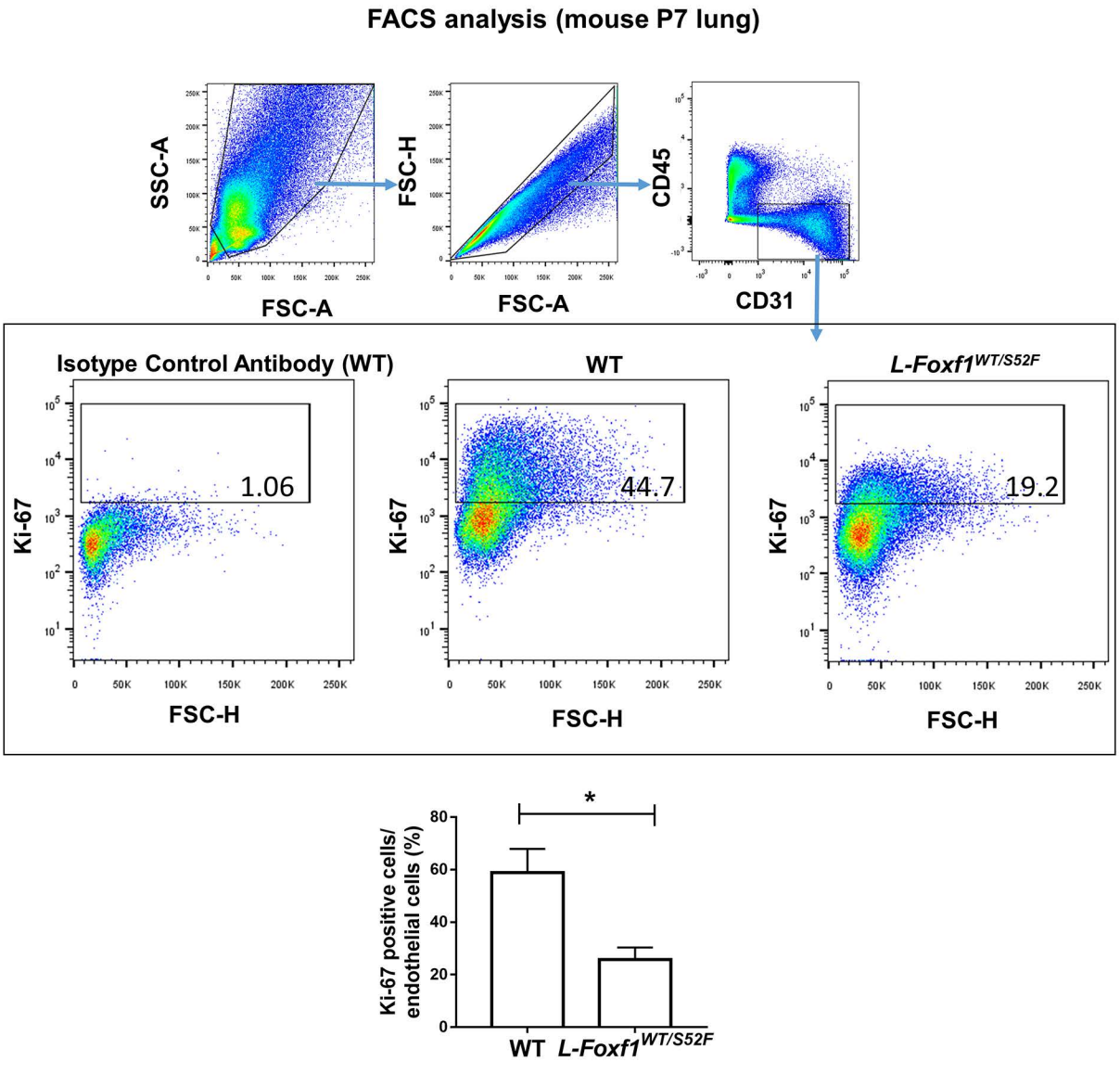
FACS analysis (mouse P7 lung)
SSC-A
FSC-A
FSC-H
FSC-A
CD45
CD31
Isotype Control Antibody (WT)
WT
L-Foxf1WT/S52F
Ki-67
FSC-H
1.06
44.7
19.2
Ki-67 positive cells/ endothelial cells (%)
*
WT
L-Foxf1WT/S52F

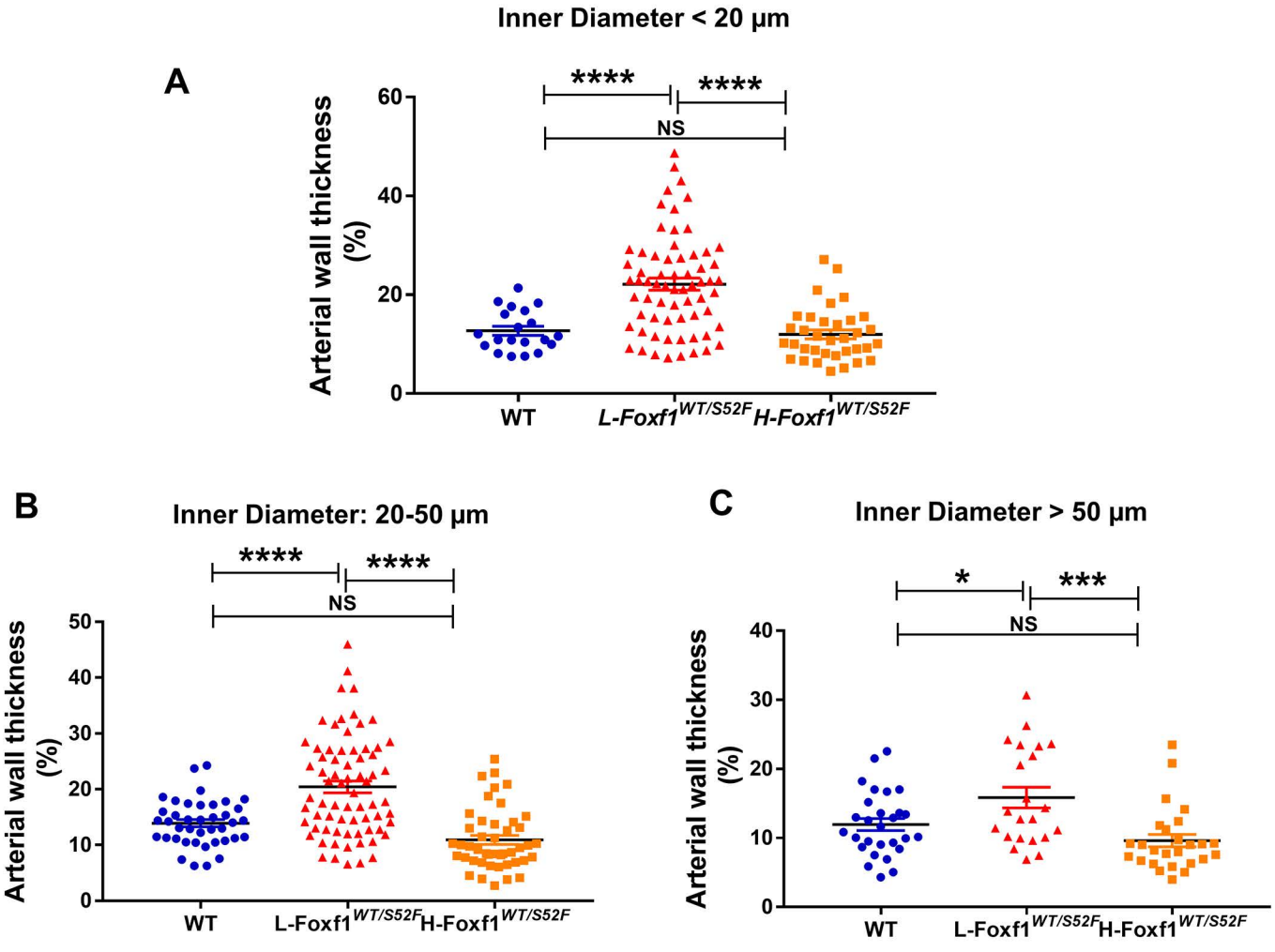

D

Mouse Genotype	WT			*L-Foxf1*$^{WT/S52F}$			*H-Foxf1*$^{WT/S52F}$		
Arterial inner diameter (μm)	<20	20-50	>50	<20	20-50	>50	<20	20-50	>50
% of non-remodeled	0.00%	0.00%	0.00%	46.97%	66.20%	27.27%	94.29%	97.78%	96.30%
% of partially remodeled	0.00%	0.00%	0.00%	53.03%	33.80%	72.73%	5.71%	2.22%	3.70%
% of fully remodeled	0.00%	0.00%	0.00%	0.00%	0.00%	0.00%	0.00%	0.00%	0.00%

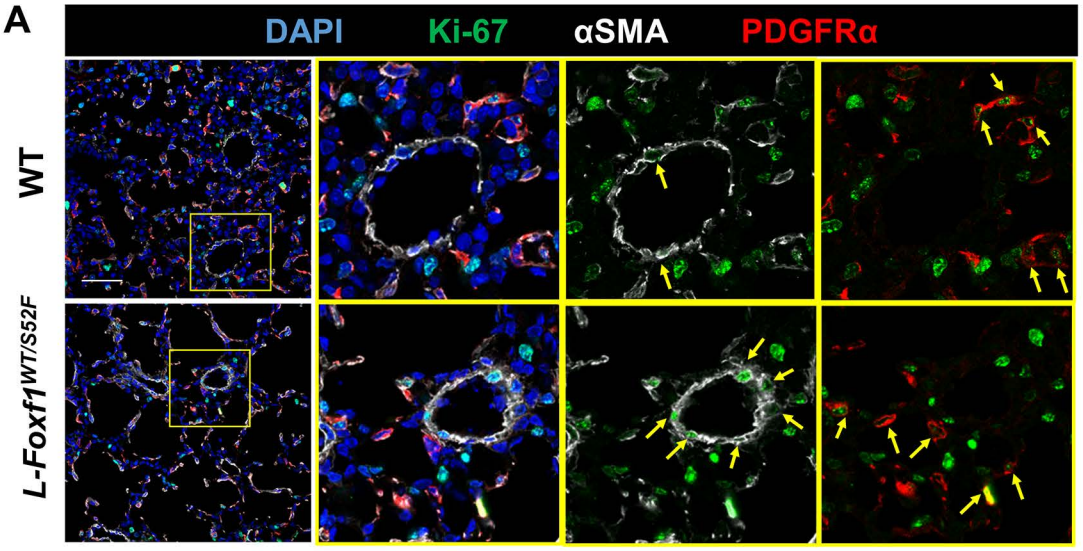
A
DAPI
Ki-67
αSMA
PDGFRα
WT
L-Foxf1WT/S52F

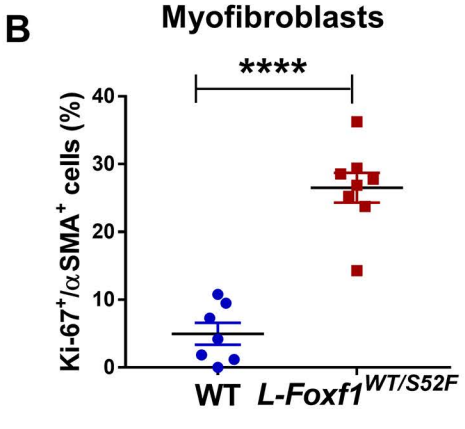
B
Myofibroblasts
****
Ki-67+/αSMA+ cells (%)
40
30
20
10
0
WT
L-Foxf1WT/S52F

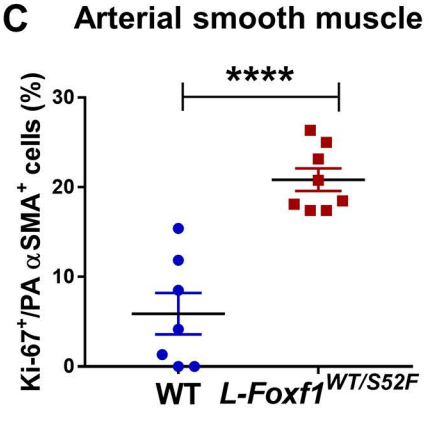
C
Arterial smooth muscle cells
****
Ki-67+/PA αSMA+ cells (%)
30
20
10
0
WT
L-Foxf1WT/S52F

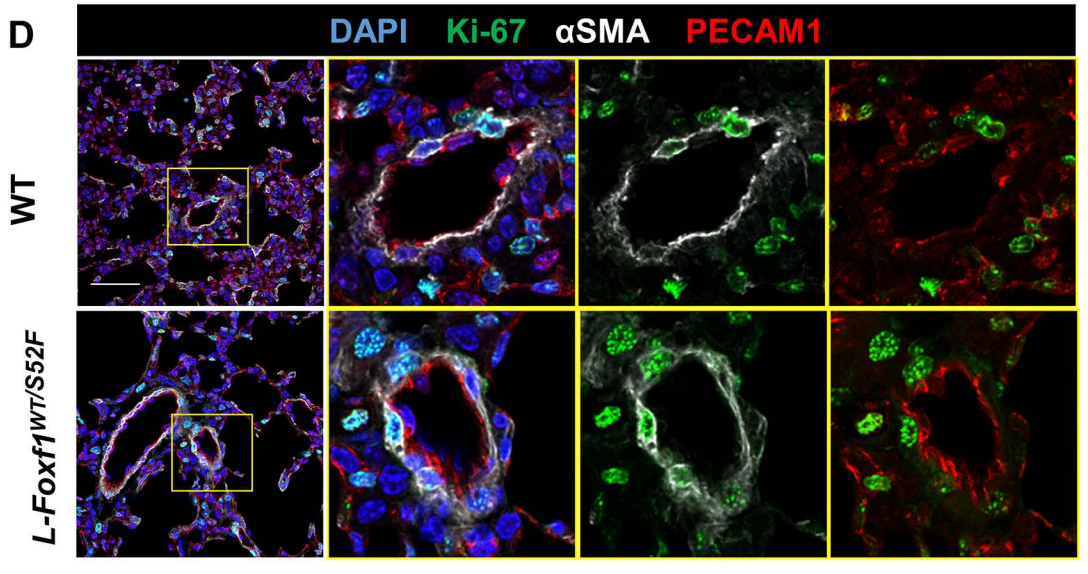
D
DAPI
Ki-67
αSMA
PECAM1
WT
L-Foxf1WT/S52F

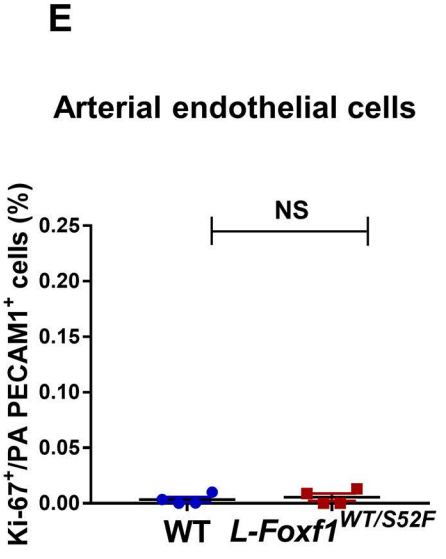
E
Arterial endothelial cells
NS
Ki-67+/PA PECAM1+ cells (%)
0.25
0.20
0.15
0.10
0.05
0.00
WT
L-Foxf1WT/S52F

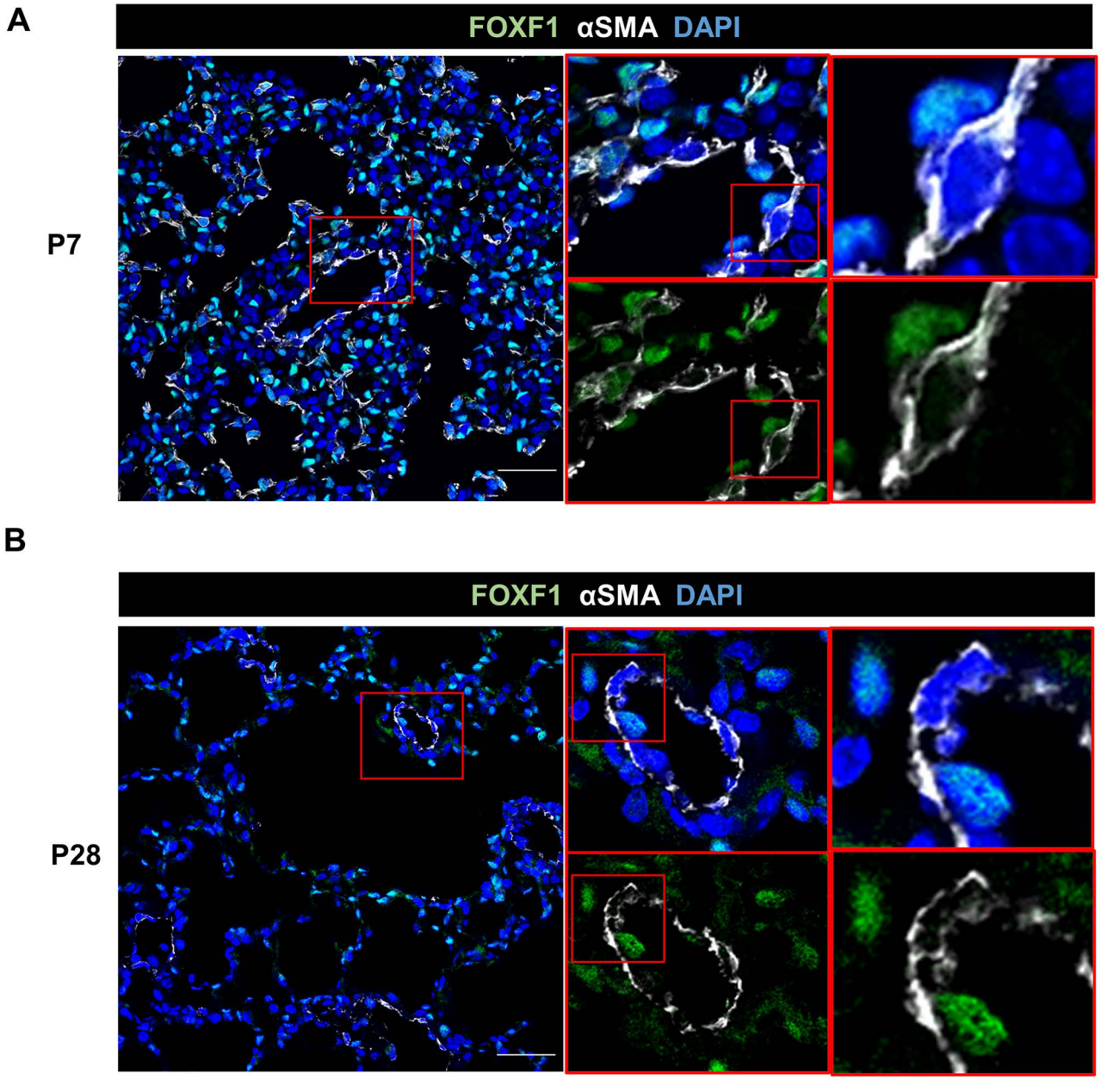
A
FOXF1 αSMA DAPI
P7
B
FOXF1 αSMA DAPI
P28

Donor

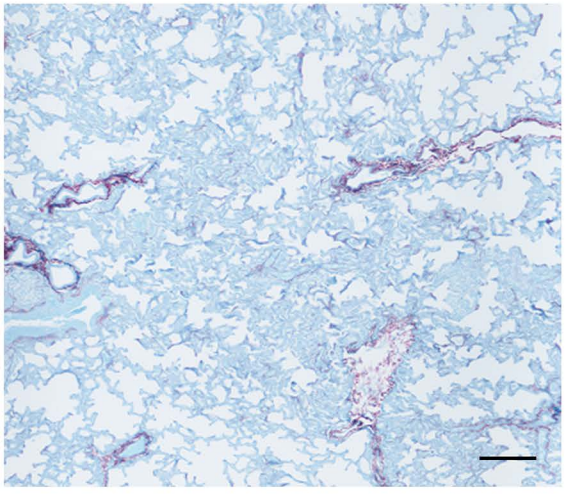

ACDMPV Patient1

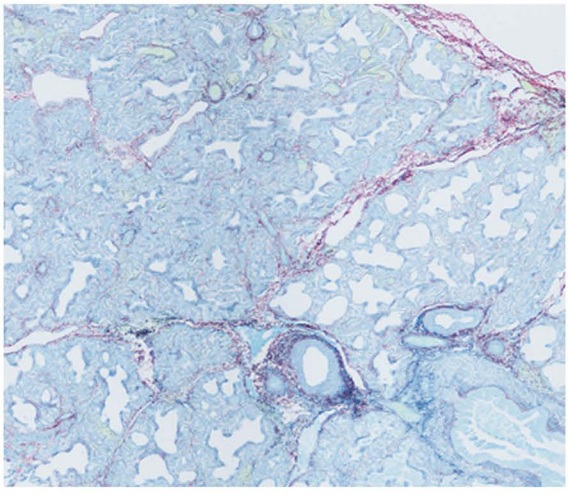

ACDMPV Patient2

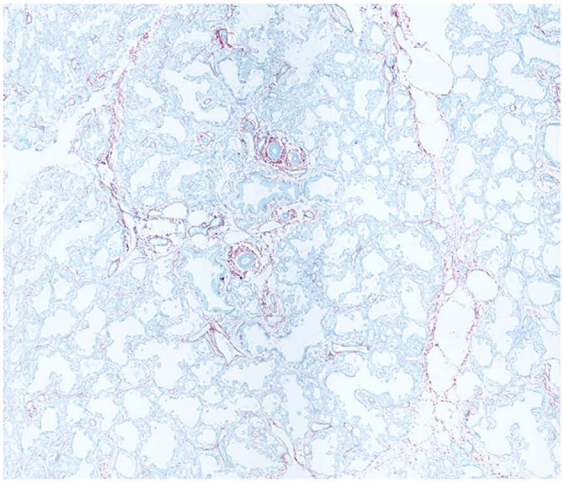

ACDMPV Patient3

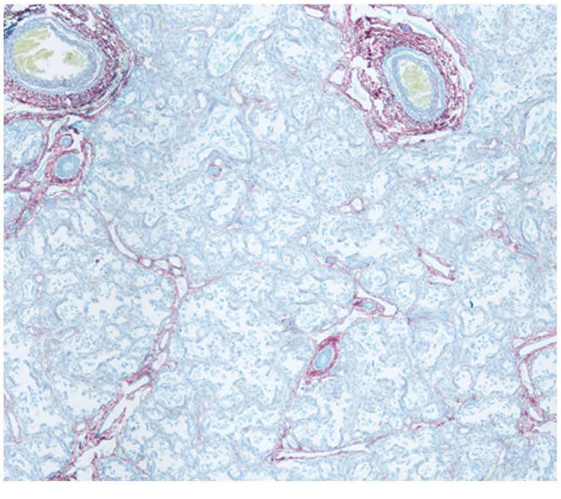

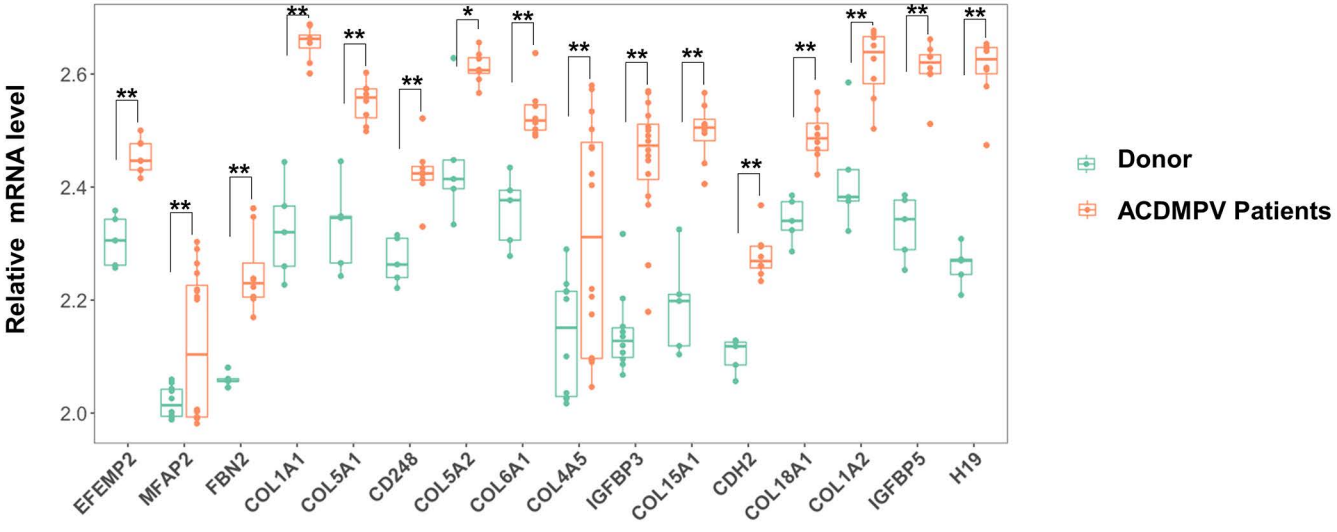
Relative mRNA level
2.0
2.2
2.4
2.6
EFEMP2
MFAP2
FBN2
COL1A1
COL5A1
CD248
COL5A2
COL6A1
COL4A5
IGFBP3
COL15A1
CDH2
COL18A1
COL1A2
IGFBP5
H19
Donor
ACDMPV Patients

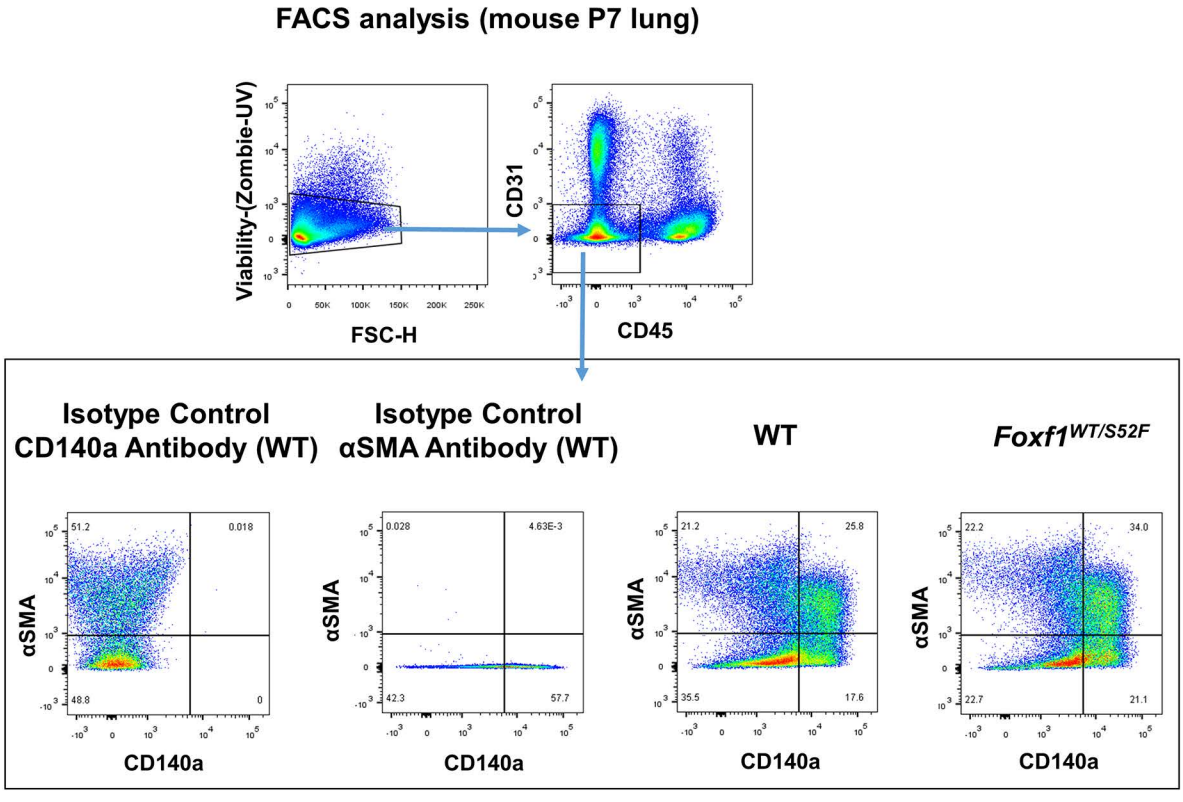
FACS analysis (mouse P7 lung)
Viability-(Zombie-UV)
FSC-H
CD31
CD45
Isotype Control
CD140a Antibody (WT)
Isotype Control
αSMA Antibody (WT)
WT
Foxf1WT/S52F
αSMA
CD140a
51.2
0.018
48.8
0
0.028
4.63E-3
42.3
57.7
21.2
25.8
35.5
17.6
22.2
34.0
22.7
21.1

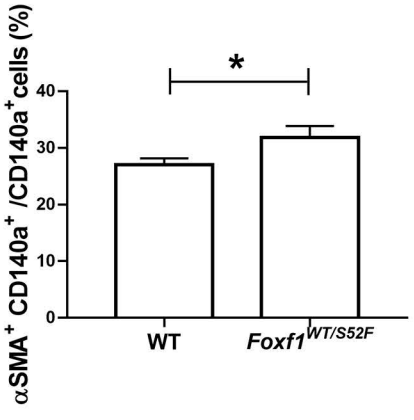
αSMA+ CD140a+ /CD140a+cells (%)
*
WT
Foxf1WT/S52F

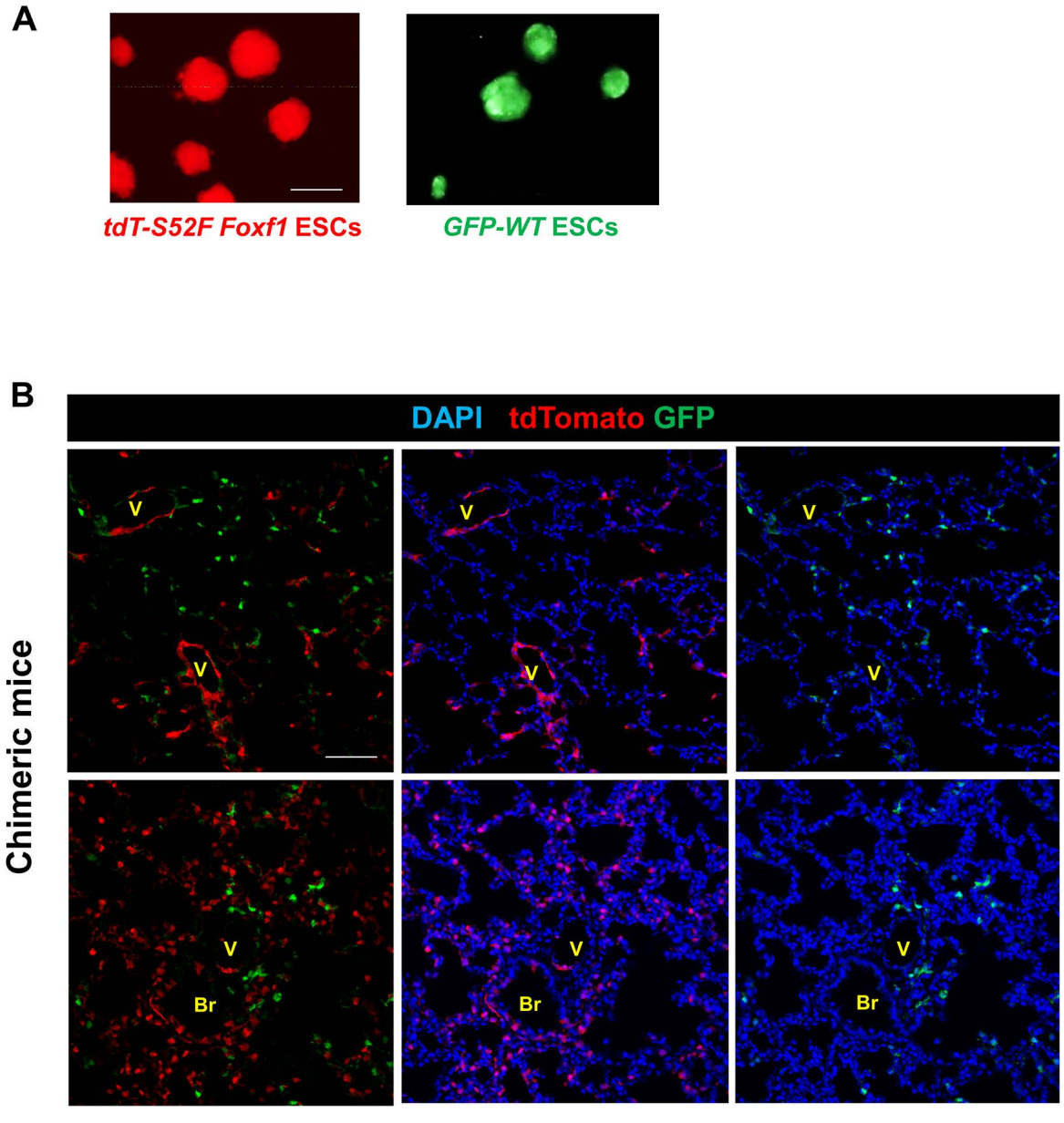
A
tdT-S52F Foxf1 ESCs
GFP-WT ESCs
B
DAPI tdTomato GFP
Chimeric mice
V
Br

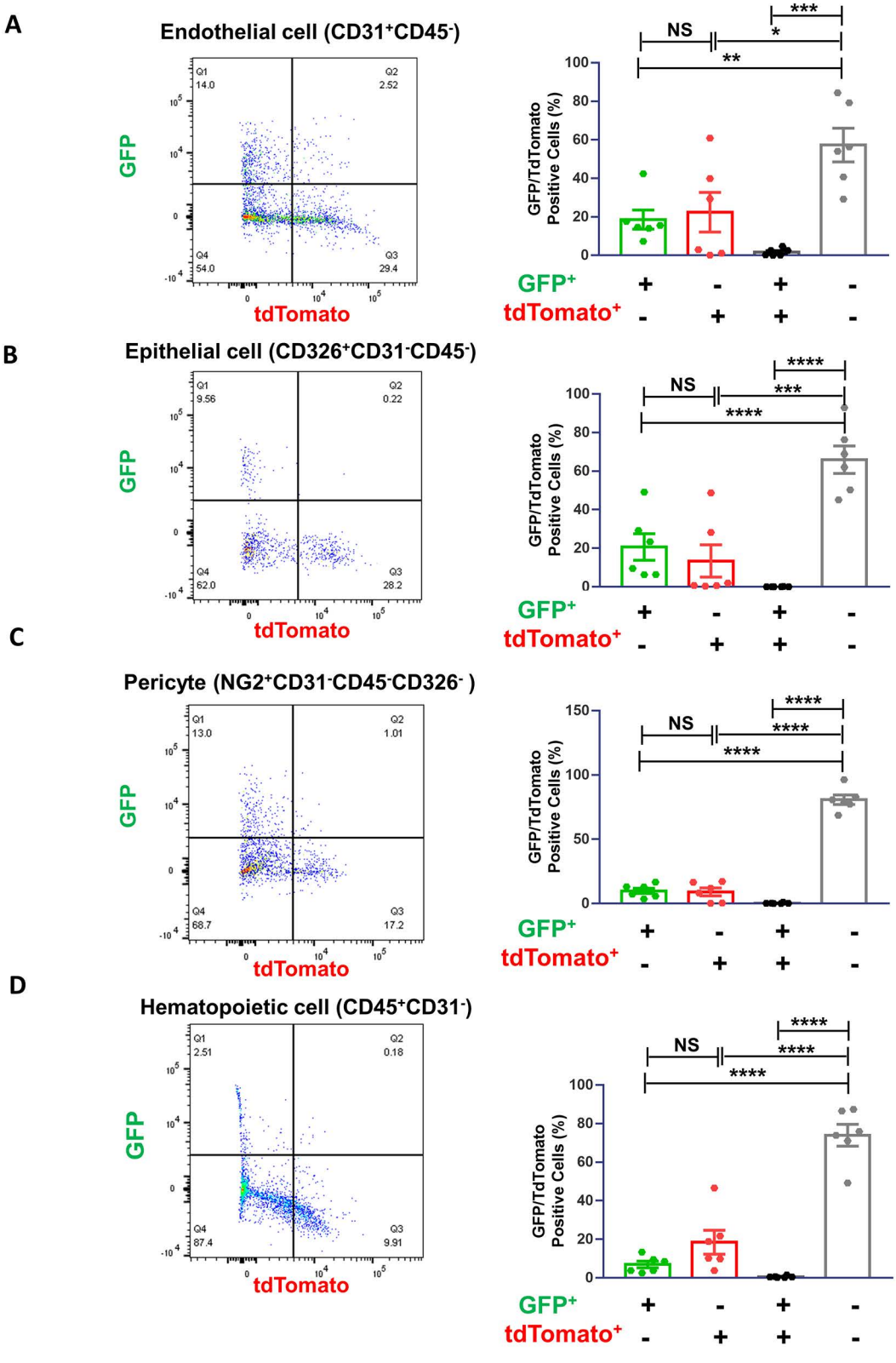
A
Endothelial cell (CD31+CD45-)
GFP
tdTomato
Q1 14.0
Q2 2.52
Q4 54.0
Q3 29.4
GFP/TdTomato Positive Cells (%)
NS
*
**
***
GFP+
tdTomato+
B
Epithelial cell (CD326+CD31-CD45-)
Q1 9.56
Q2 0.22
Q4 62.0
Q3 28.2
NS
***
****
C
Pericyte (NG2+CD31-CD45-CD326-)
Q1 13.0
Q2 1.01
Q4 68.7
Q3 17.2
D
Hematopoietic cell (CD45+CD31-)
Q1 2.51
Q2 0.18
Q4 87.4
Q3 9.91

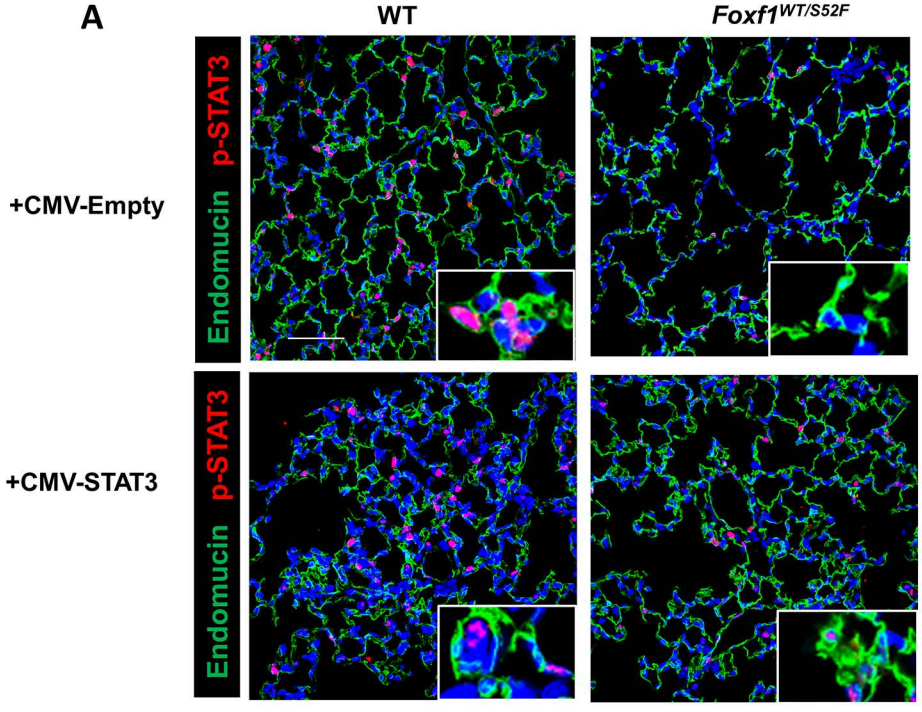
A
WT
Foxf1WT/S52F
+CMV-Empty
+CMV-STAT3
Endomucin
p-STAT3

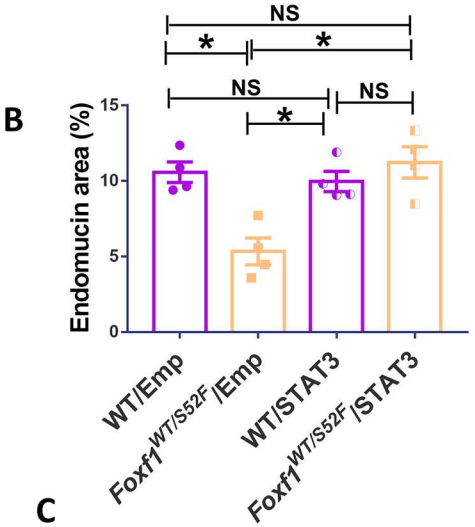
B
Endomucin area (%)
NS
*
NS
*
NS
*
NS
WT/Emp
Foxf1WT/S52F/Emp
WT/STAT3
Foxf1WT/S52F/STAT3

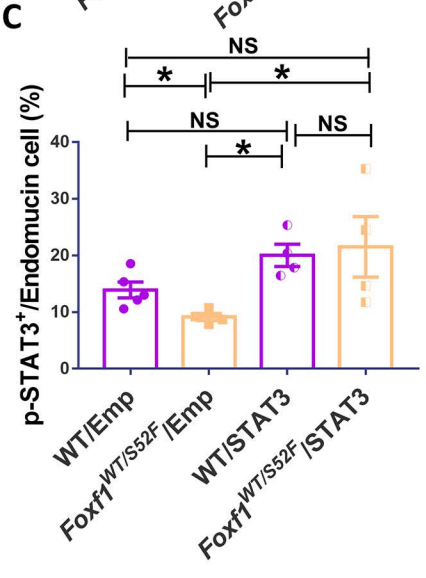
C
p-STAT3+/Endomucin cell (%)
NS
*
NS
*
NS
*
NS
WT/Emp
Foxf1WT/S52F/Emp
WT/STAT3
Foxf1WT/S52F/STAT3

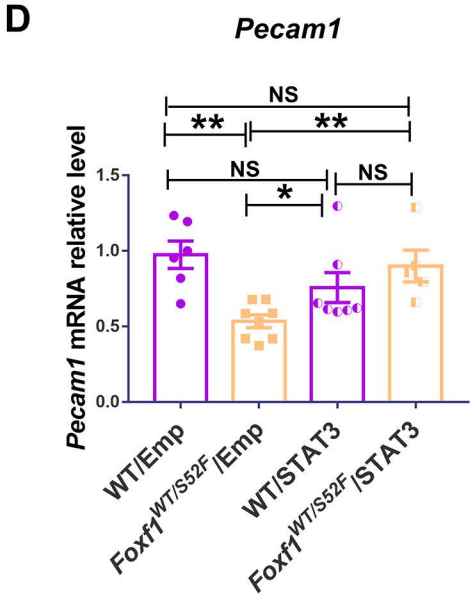
D
Pecam1
Pecam1 mRNA relative level
NS
**
**
NS
*
NS
WT/Emp
Foxf1WT/S52F/Emp
WT/STAT3
Foxf1WT/S52F/STAT3

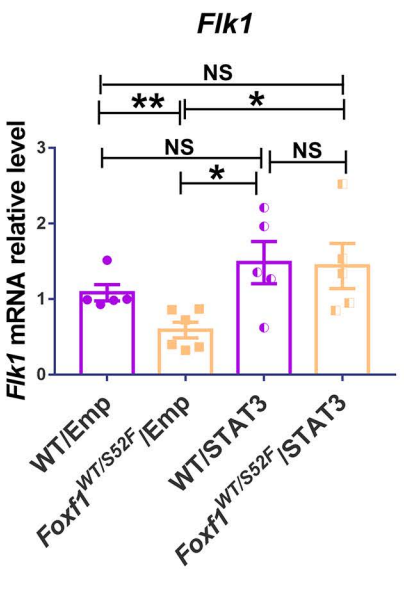
E
Flk1
Flk1 mRNA relative level
NS
**
*
NS
*
NS
WT/Emp
Foxf1WT/S52F/Emp
WT/STAT3
Foxf1WT/S52F/STAT3

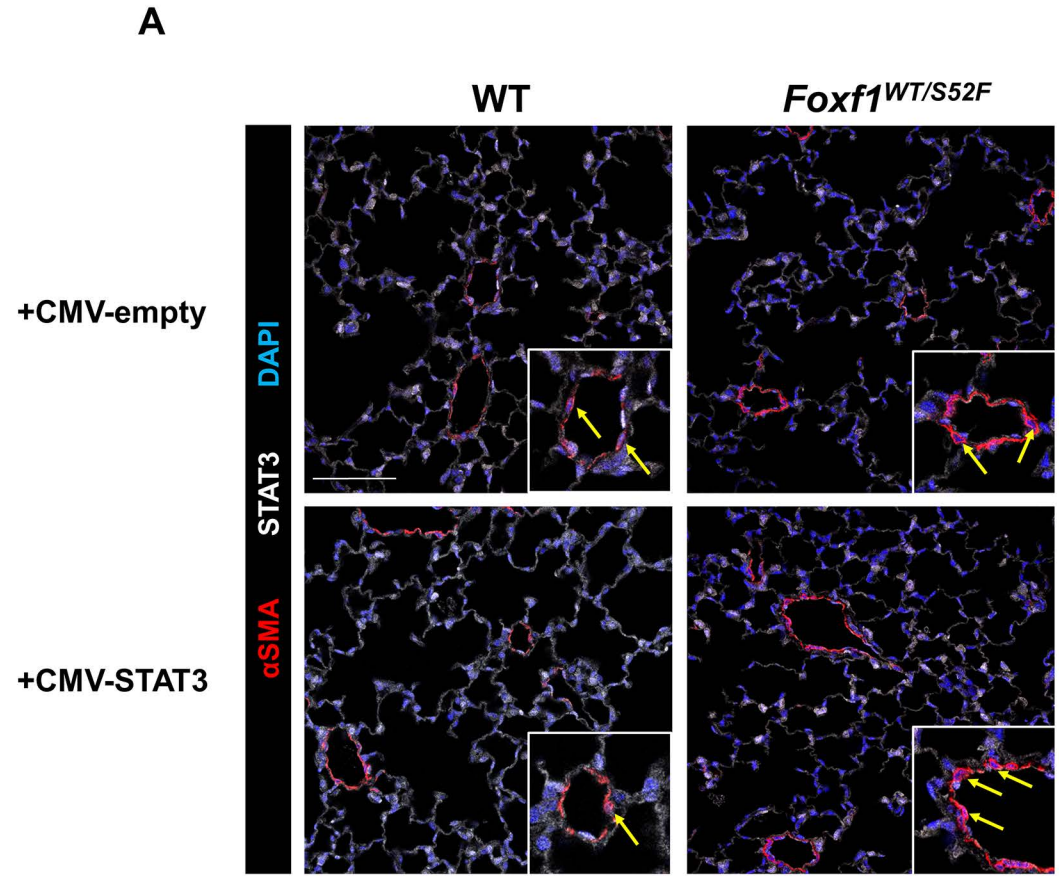
A
WT
Foxf1WT/S52F
+CMV-empty
+CMV-STAT3
DAPI
STAT3
αSMA

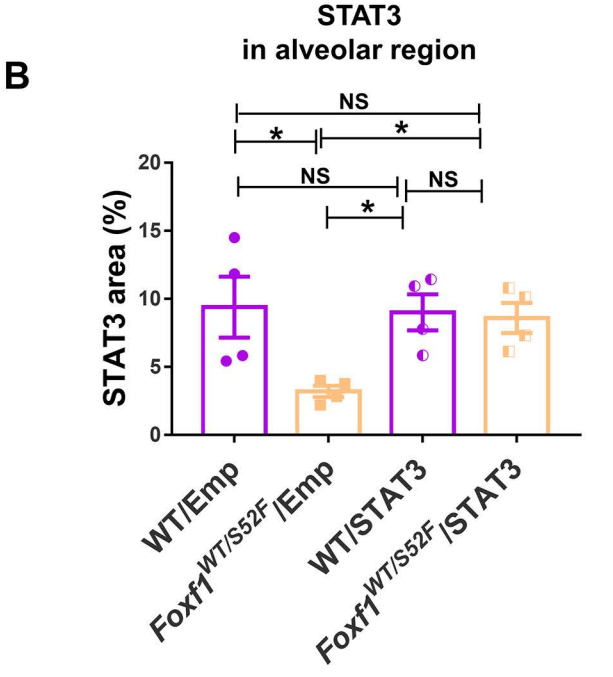
B
STAT3
in alveolar region
STAT3 area (%)
NS
*
*
NS
NS
*
WT/Emp
Foxf1WT/S52F /Emp
WT/STAT3
Foxf1WT/S52F /STAT3

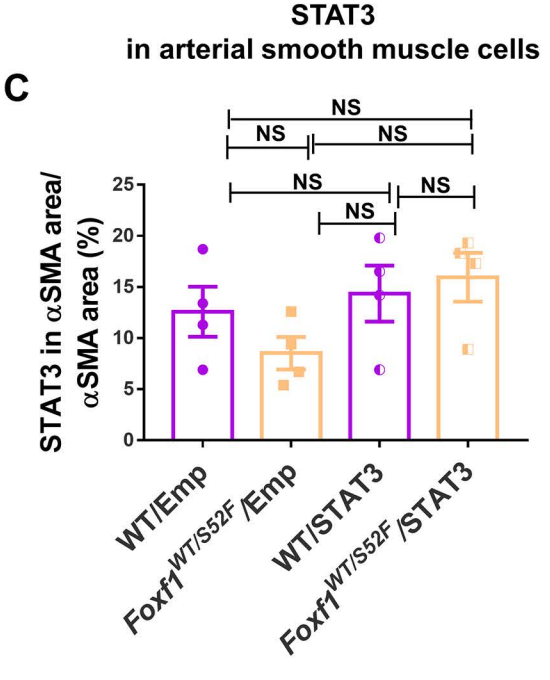
C
STAT3
in arterial smooth muscle cells
STAT3 in αSMA area/
αSMA area (%)
NS
NS
NS
NS
NS
NS
WT/Emp
Foxf1WT/S52F /Emp
WT/STAT3
Foxf1WT/S52F /STAT3

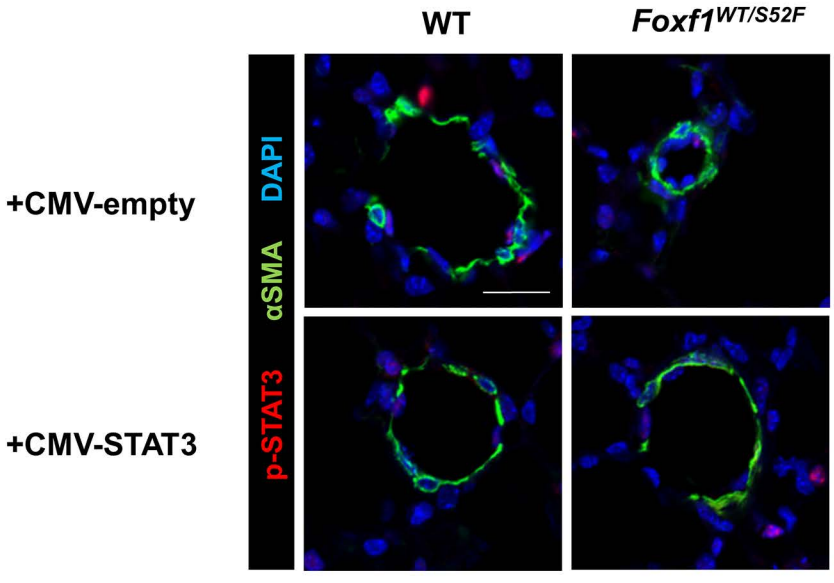
WT
Foxf1WT/S52F
+CMV-empty
+CMV-STAT3
DAPI
αSMA
p-STAT3

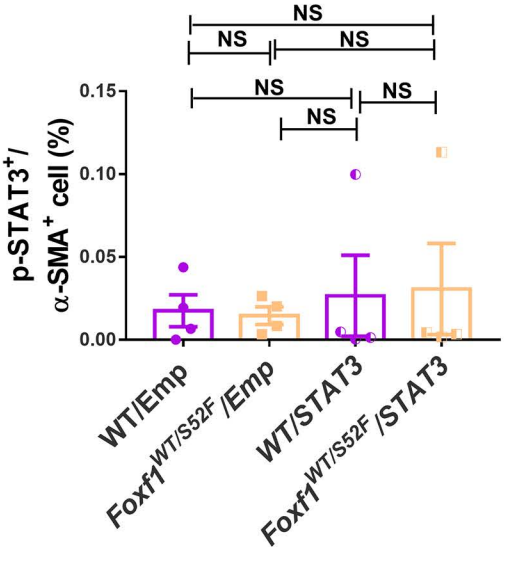
NS
NS
NS
NS
NS
NS
0.15
0.10
0.05
0.00
p-STAT3+/
α-SMA+ cell (%)
WT/Emp
Foxf1WT/S52F /Emp
WT/STAT3
Foxf1WT/S52F /STAT3

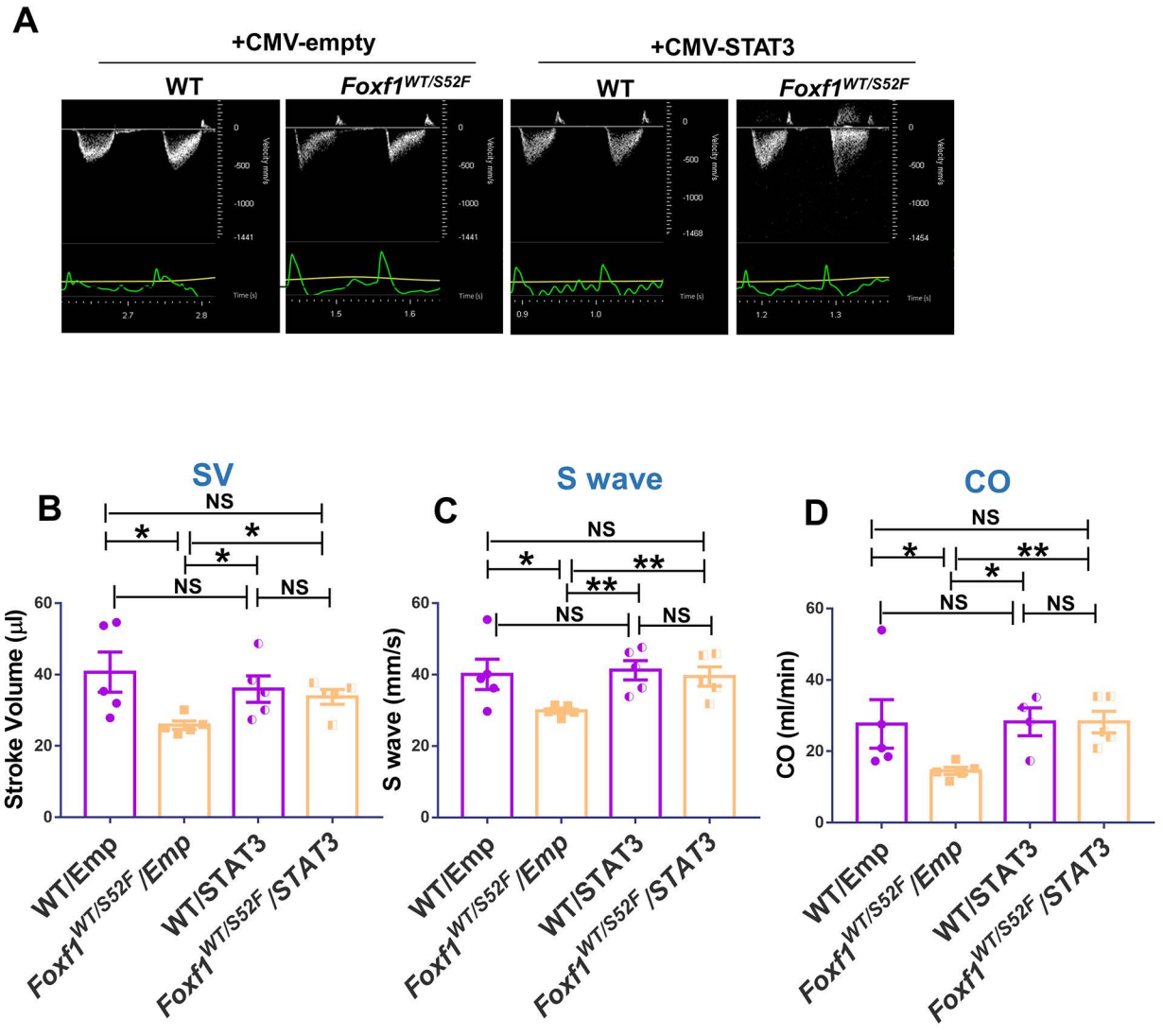
A
+CMV-empty
+CMV-STAT3
WT
Foxf1WT/S52F
WT
Foxf1WT/S52F
B
SV
Stroke Volume (μl)
C
S wave
S wave (mm/s)
D
CO
CO (ml/min)
NS
*
**
WT/Emp
Foxf1WT/S52F /Emp
WT/STAT3
Foxf1WT/S52F /STAT3

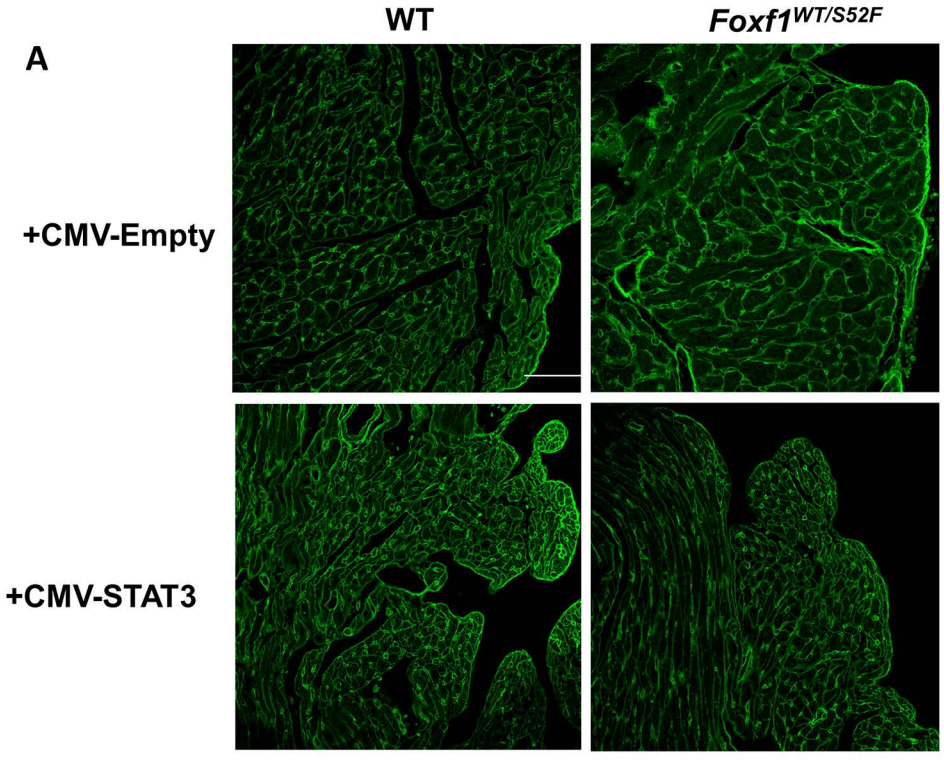
A
WT
Foxf1WT/S52F
+CMV-Empty
+CMV-STAT3

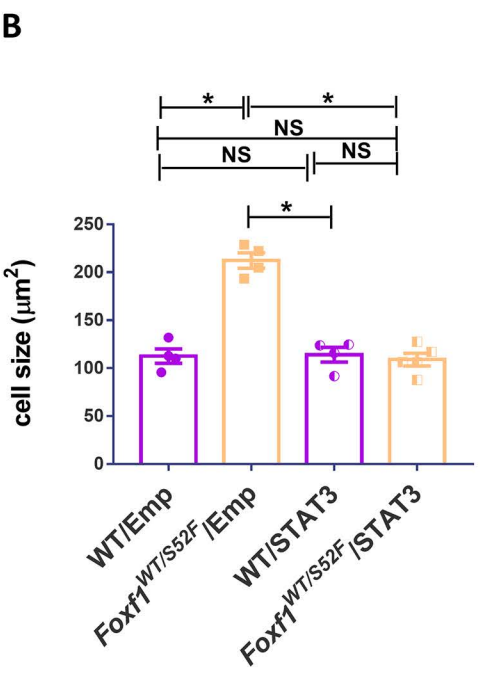
B
*
*
NS
NS
NS
*
cell size (μm2)
250
200
150
100
50
0
WT/Emp
Foxf1WT/S52F/Emp
WT/STAT3
Foxf1WT/S52F/STAT3

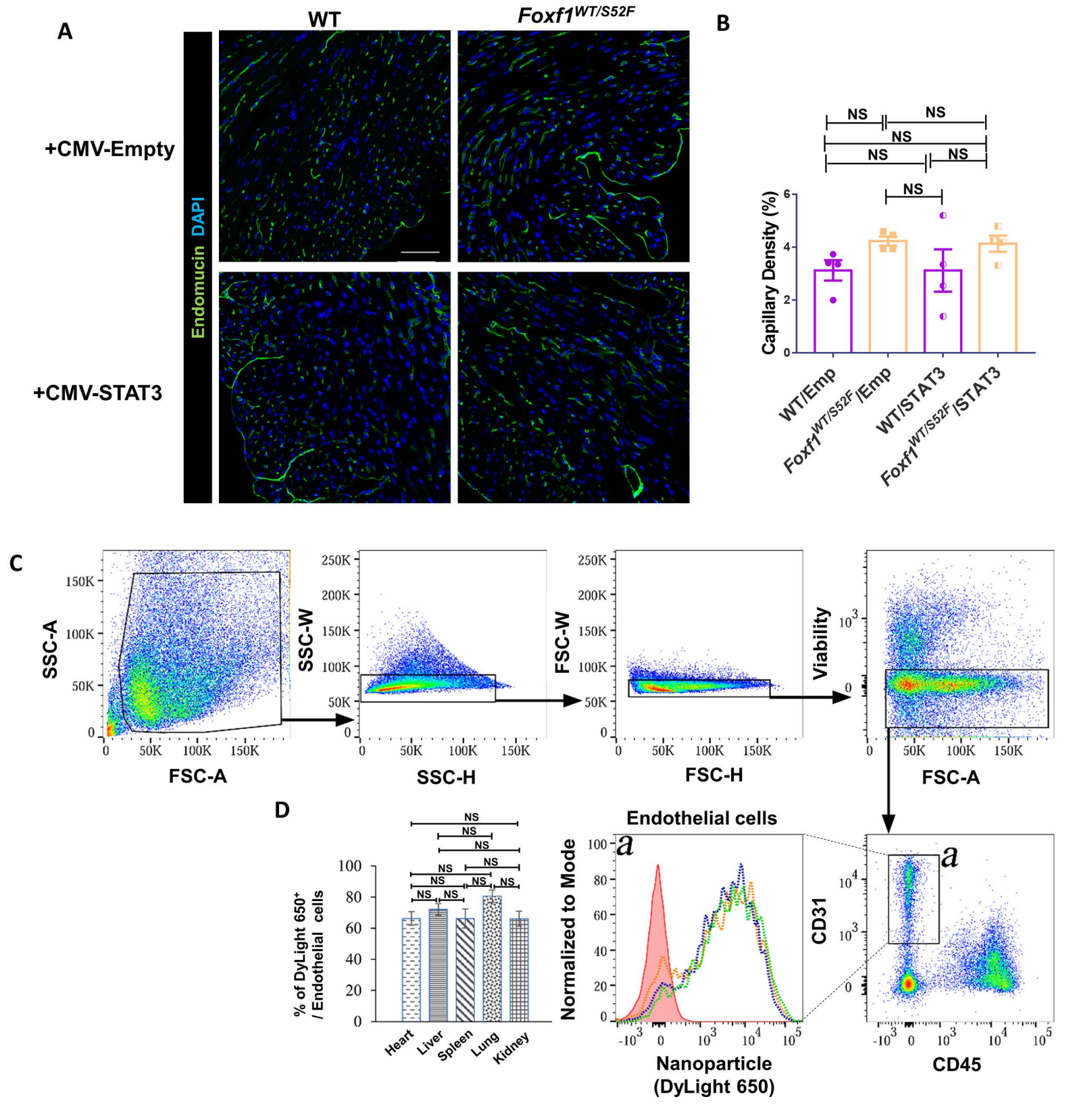
A
WT
Foxf1WT/S52F
+CMV-Empty
+CMV-STAT3
Endomucin DAPI
B
NS
Capillary Density (%)
WT/Emp
Foxf1WT/S52F/Emp
WT/STAT3
Foxf1WT/S52F/STAT3
C
SSC-A
FSC-A
SSC-W
SSC-H
FSC-W
FSC-H
Viability
FSC-A
D
% of DyLight 650+ / Endothelial cells
Heart
Liver
Spleen
Lung
Kidney
Endothelial cells
Normalized to Mode
Nanoparticle (DyLight 650)
CD31
CD45

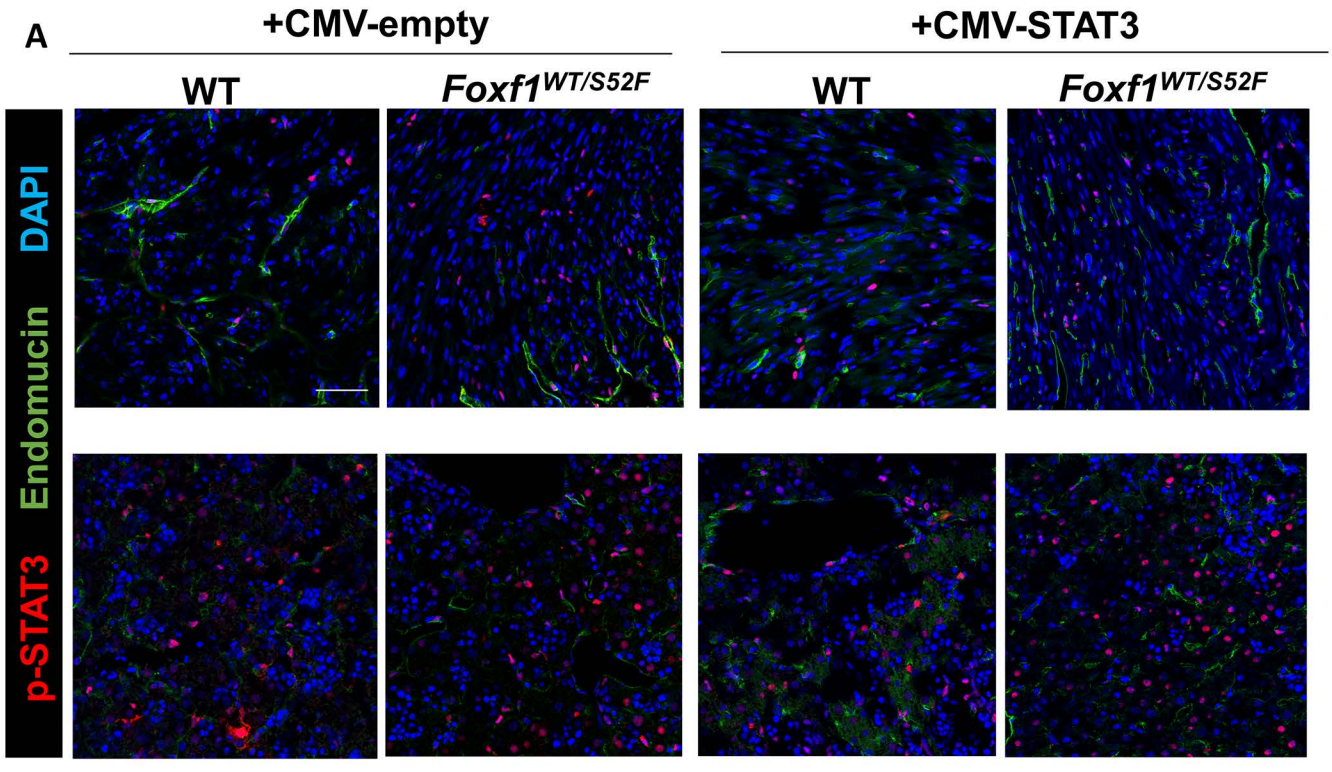
A
+CMV-empty
+CMV-STAT3
WT
Foxf1WT/S52F
WT
Foxf1WT/S52F
Heart
Liver
DAPI
Endomucin
p-STAT3

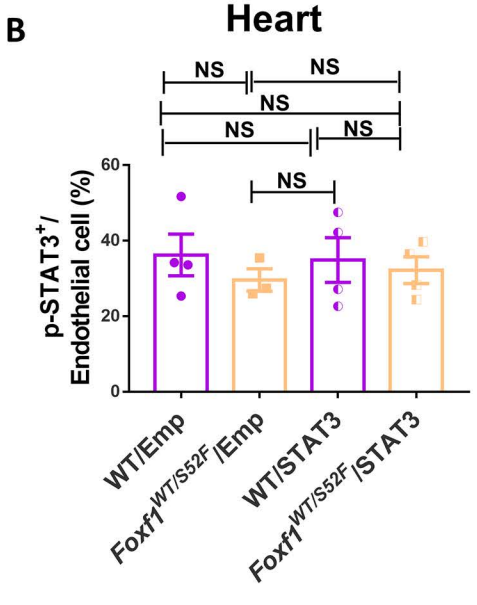
B
Heart
NS
NS
NS
NS
NS
NS
p-STAT3+/ Endothelial cell (%)
60
40
20
0
WT/Emp
Foxf1WT/S52F/Emp
WT/STAT3
Foxf1WT/S52F/STAT3

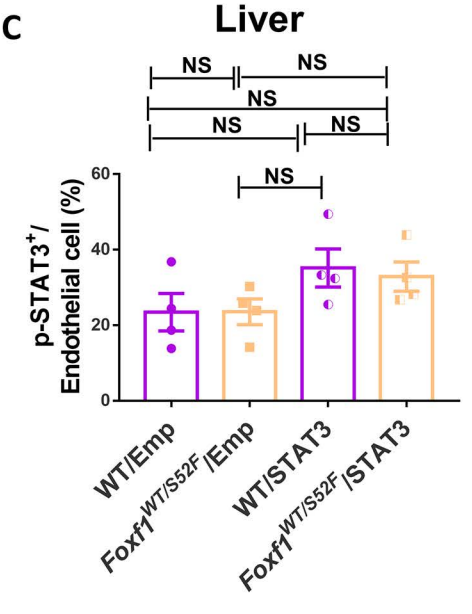
C
Liver
NS
NS
NS
NS
NS
NS
p-STAT3+/ Endothelial cell (%)
60
40
20
0
WT/Emp
Foxf1WT/S52F/Emp
WT/STAT3
Foxf1WT/S52F/STAT3

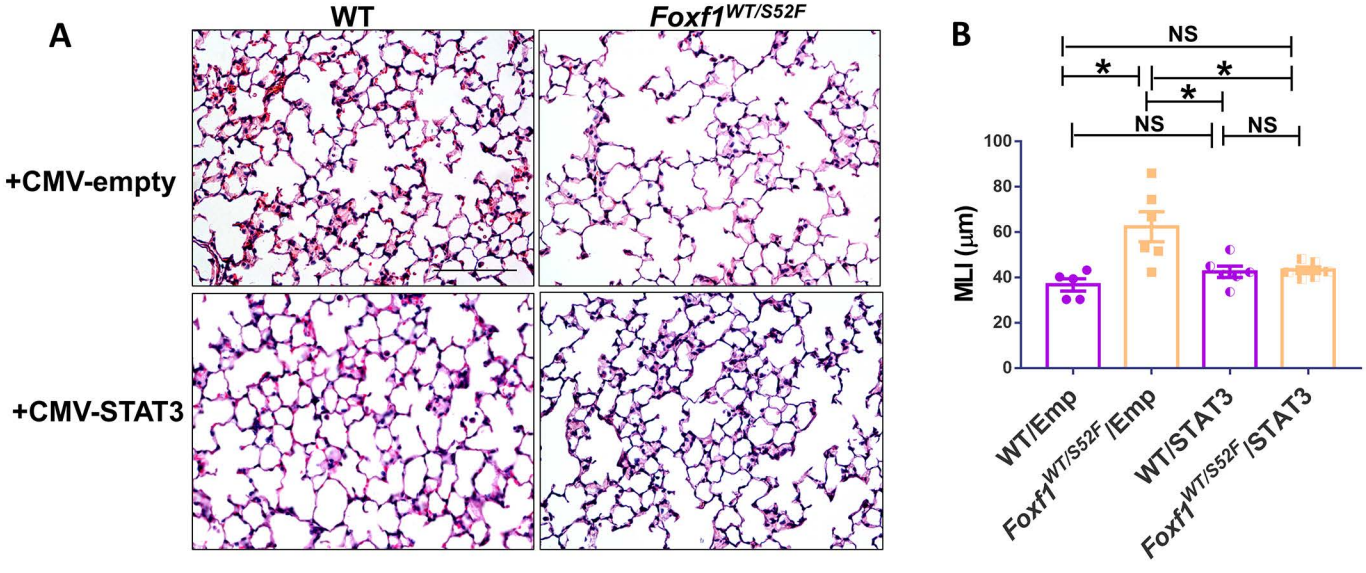
A
WT
Foxf1WT/S52F
+CMV-empty
+CMV-STAT3
B
NS
*
*
*
NS
NS
MLI (μm)
100
80
60
40
20
0
WT/Emp
Foxf1WT/S52F/Emp
WT/STAT3
Foxf1WT/S52F/STAT3

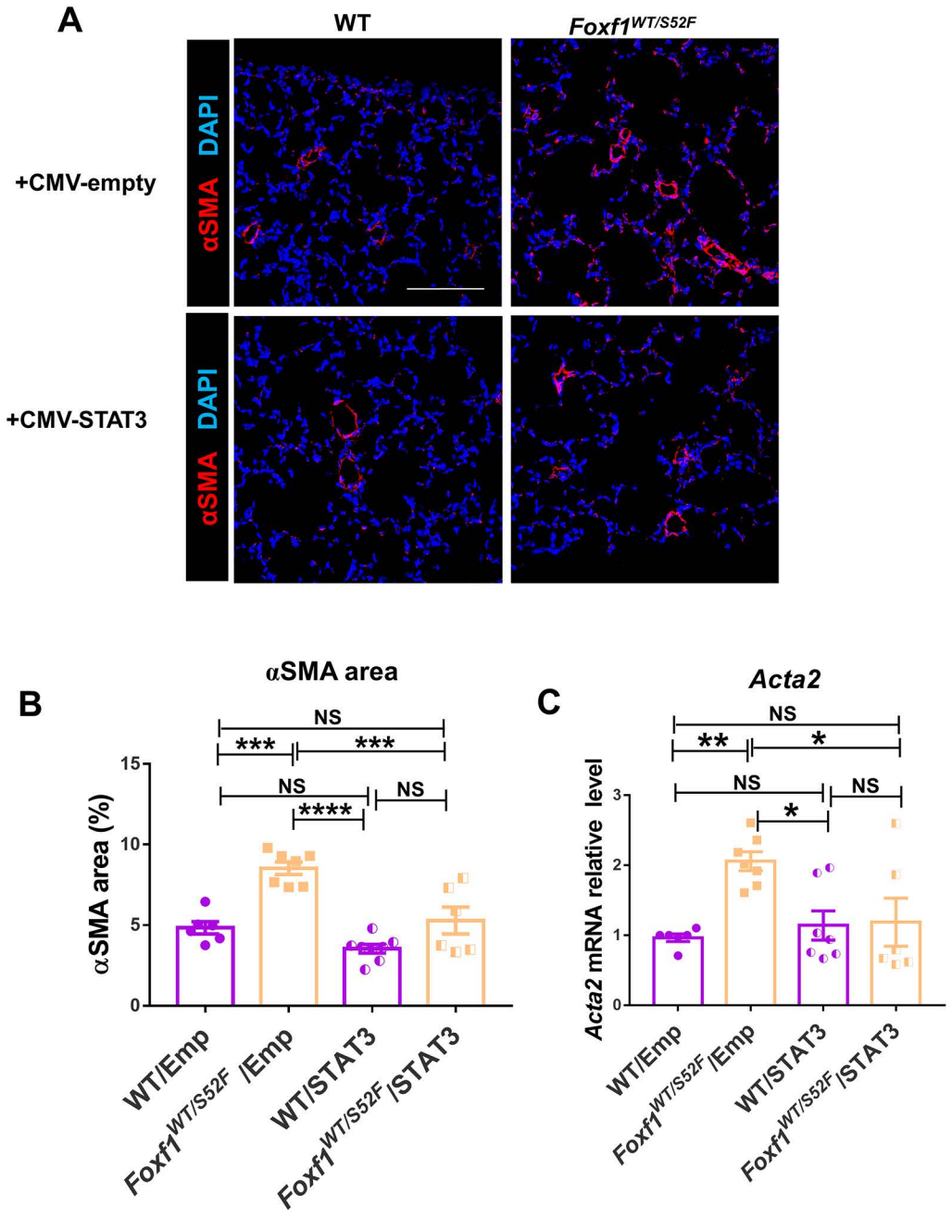
A
WT
Foxf1WT/S52F
+CMV-empty
+CMV-STAT3
αSMA DAPI
αSMA DAPI
B
αSMA area
αSMA area (%)
NS
***
***
NS
NS
****
WT/Emp
Foxf1WT/S52F /Emp
WT/STAT3
Foxf1WT/S52F /STAT3
C
Acta2
Acta2 mRNA relative level
NS
**
*
NS
NS
*
WT/Emp
Foxf1WT/S52F /Emp
WT/STAT3
Foxf1WT/S52F /STAT3

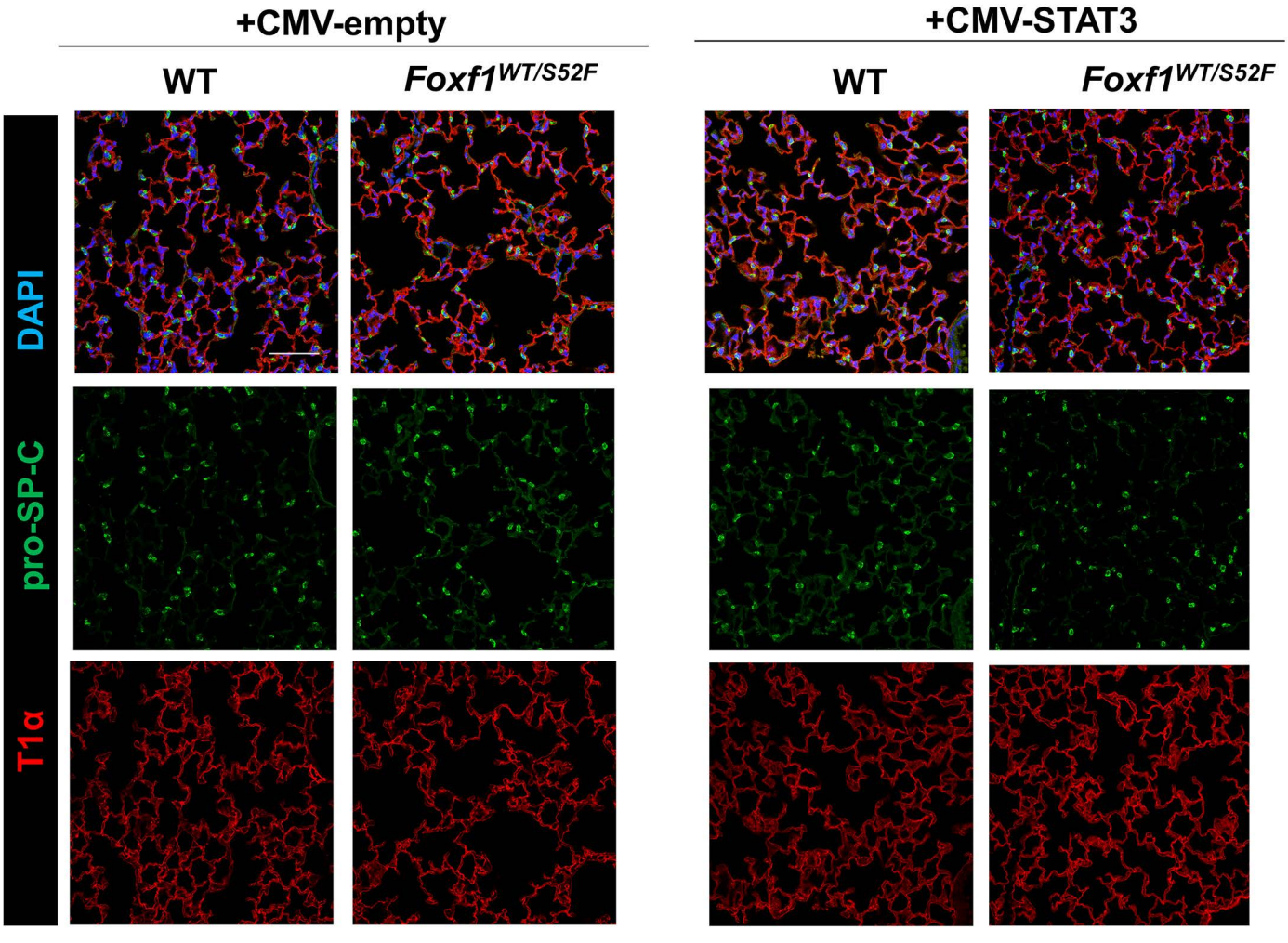
+CMV-empty
+CMV-STAT3
WT
Foxf1WT/S52F
WT
Foxf1WT/S52F
DAPI
pro-SP-C
T1α

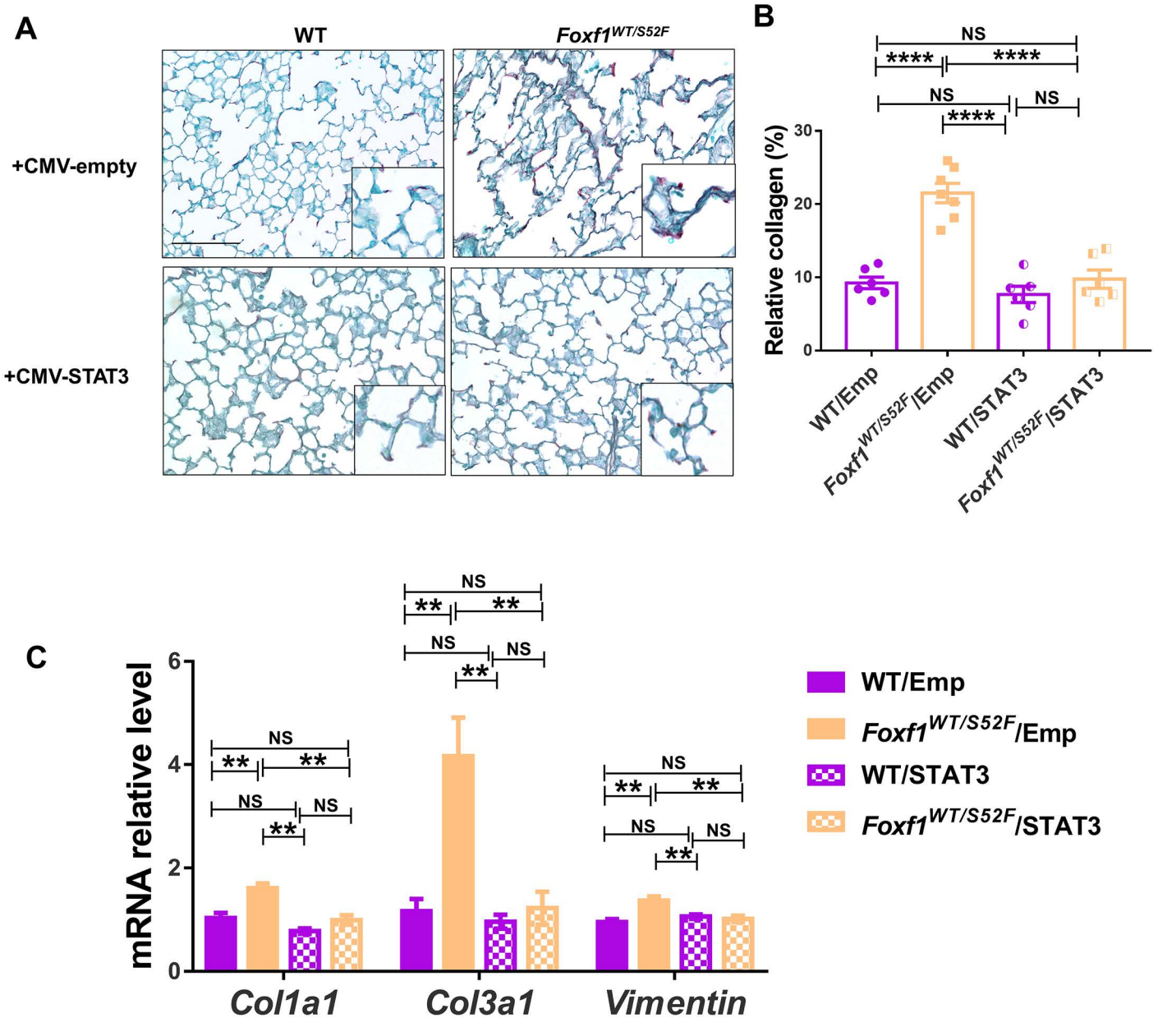
A
WT
Foxf1WT/S52F
+CMV-empty
+CMV-STAT3
B
Relative collagen (%)
NS
****
****
NS
NS
****
30
20
10
0
WT/Emp
Foxf1WT/S52F/Emp
WT/STAT3
Foxf1WT/S52F/STAT3
C
mRNA relative level
6
4
2
0
NS
**
**
NS
NS
**
Col1a1
Col3a1
Vimentin
WT/Emp
Foxf1WT/S52F/Emp
WT/STAT3
Foxf1WT/S52F/STAT3

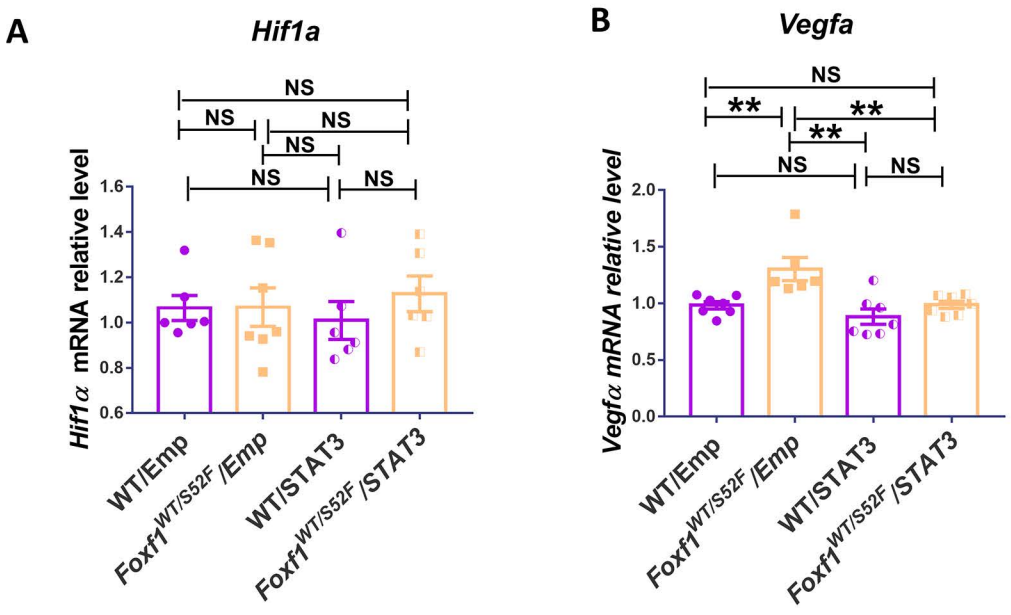
A
Hif1a
Hif1α mRNA relative level
NS
NS
NS
NS
NS
NS
1.6
1.4
1.2
1.0
0.8
0.6
WT/Emp
Foxf1WT/S52F/Emp
WT/STAT3
Foxf1WT/S52F/STAT3
B
Vegfa
Vegfα mRNA relative level
NS
**
**
**
NS
NS
2.0
1.5
1.0
0.5
0.0
WT/Emp
Foxf1WT/S52F/Emp
WT/STAT3
Foxf1WT/S52F/STAT3

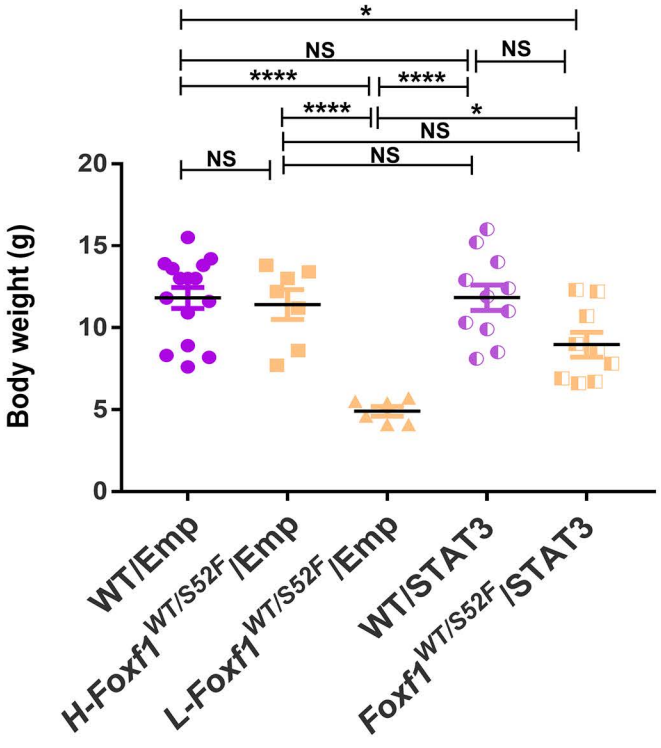
*
NS
NS
****
****
****
*
NS
NS
NS
20
15
10
5
0
Body weight (g)
WT/Emp
H-Foxf1WT/S52F/Emp
L-Foxf1WT/S52F/Emp
WT/STAT3
Foxf1WT/S52F/STAT3

A

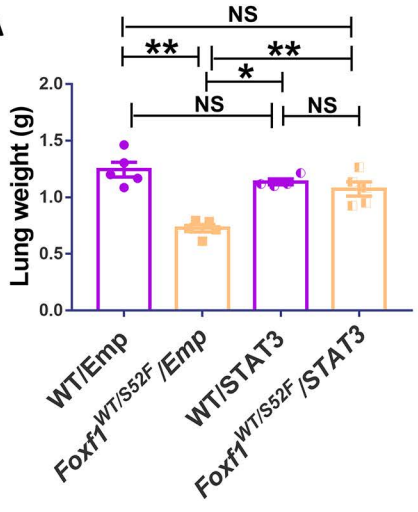

B

Treatment group	Untreated	Injected with CMV-empty		Injected with CMV-STAT3	
Mouse genotype	*Foxf1*$^{WT/S52F}$	*Foxf1*$^{WT/S52F}$	WT	*Foxf1*$^{WT/S52F}$	WT
Number of mice at P2	**366**	**10**	**18**	**23**	**35**
Number of mice at P28	**137**	**3**	**18**	**15**	**33**
% of mortality	**62.57%**	**70.00%**	**0.00%**	**34.78%**	**5.71%**

SUPPLEMENTAL FIGURE LEGENDS

Supplemental Figure I. Genotyping and echocardiography in adult *Foxf1*$^{WT/S52F}$ mice. (A) Nucleotide sequences of the *WT Foxf1* and *S52F Foxf1* mutant alleles. (B) PCR shows genotyping of *WT* and *Foxf1*$^{WT/S52F}$ mice. Mutant PCR product is indicated with red arrow. (C-D) Echocardiography of adult *Foxf1*$^{WT/S52F}$ mice shows increased diastolic (d) and systolic (s) right ventricular (RV) chamber area in apical and short axis (SX) view (n=6-10 mice per group). Compared to *WT* controls, *Foxf1*$^{WT/S52F}$ mice exhibit increased left ventricular (LV) internal diameter and LV volume at the end of diastole (LVID;d and LV Vol;d). There are no changes in interventricular septal thickness at diastole (IVS;d), interventricular septal thickness at systole (IVS;s), left atrium (LA) diameter, left ventricular internal diameter at the end of systole (LVID;s), left ventricular posterior wall thickness at the end of diastole (LVPW;d), left ventricular posterior wall thickness at the end of systole (LVPW;s), left ventricular mass (LV Mass) and left ventricular volume at the end of systole (LV Vol;s). * indicates $p < 0.05$.

Supplemental Figure II. *Foxf1*$^{WT/S52F}$ adult mice exhibit enlarged hearts. (A) Photograph shows an enlarged heart of *Foxf1*$^{WT/S52F}$ mouse compared to *WT* control. (B) Photograph shows no significant difference (NS) in the body weight between *Foxf1*$^{WT/S52F}$ and *WT* mice（n=8-11 mice per group). (C) The ratio of heart weight to body weight is higher in *Foxf1*$^{WT/S52F}$ mice compared to *WT* littermates (n=4-5 mice per group). (D-H) qRT-PCR shows that *Nppa*, *Nppb* and *Myh7* mRNAs, and the *Myh7*/*Myh6* ratio are increased in right ventricles of *Foxf1*$^{WT/S52F}$ mice. There are no significant changes in *Myh6* mRNA between *Foxf1*$^{WT/S52F}$ and *WT* hearts. mRNAs were normalized using *β-actin* mRNA (n=6-10 mice per group). (I-J) Wheat germ agglutinin (WGA) staining of heart sections shows no significant difference in the size of left ventricular (LV) cardiomyocytes between *Foxf1*$^{WT/S52F}$ and *WT* mice. Five random lung images per mouse (n=6 mice per group) were used for quantification. Scale bars are 100μm. (K) Sirius red staining of heart sections shows collagen depositions

(red) in the right ventricle (RV). No visual difference is seen in collagen deposition in RV myocardium between *Foxf1*$^{WT/S52F}$ and WT mice. Scale bars are 50μm.

Supplemental Figure III. FOXF1 is not expressed in the myocardium. (A) Immunostaining for FOXF1 and Endomucin shows that FOXF1 (red) is expressed in the lung tissue (bottom panels) but not in RV myocardium of P28 *WT* mice (upper panels). Endomucin (green) is expressed in both cardiac and pulmonary endothelial cells. Sections were counterstained with DAPI (blue). Scale bars are 100μm. (B-D) Measurements of arterial wall thickness in the lung tissue show that remodeling of small (inner diameter < 20μm), medium (inner diameter = 20-50μm) and large (inner diameter > 50μm) pulmonary arteries is increased in adult *Foxf1*$^{WT/S52F}$ mice. Five random lung images per mouse were used to quantify the data (n=6-7 mice per group). (E) Table shows the percentage of remodeled pulmonary arteries in *Foxf1*$^{WT/S52F}$ and *WT* mice. * indicates $p < 0.05$, ** indicates $p < 0.01$, **** indicates $p < 0.0001$.

Supplemental Figure IV. *Foxf1*$^{WT/S52F}$ lungs exhibit reduced expression of STAT3. (A-D) Western blot shows reduced STAT3 and p-STAT3 protein levels in lungs of *Foxf1*$^{WT/S52F}$ mice at P5. There is no significant difference in the p-STAT3/STAT3 ratio between *Foxf1*$^{WT/S52F}$ and *WT* littermates. Proteins were normalized using β-actin (n=3-6 mice per group). (E-F) Immunostaining for STAT3 and Endomucin shows that STAT3 expression is decreased in lungs of *Foxf1*$^{WT/S52F}$ mice. Arrows point to nuclei of endothelial cells. Five random lung images per mouse were used to quantify the data (n=4-5 mice per group). Scale bars are 50μm. NS indicates no significant difference, * indicates $p < 0.05$.

Supplemental Figure V. *Foxf1*$^{WT/S52F}$ lungs exhibit increased VEGFα expression. (A-B) qRT-PCR shows increased *Vegfa* mRNA but no changes in *Hif1a* mRNA in lungs of adult *Foxf1*$^{WT/S52F}$ mice compared to *WT* controls. mRNAs were normalized using *β-actin* mRNA (n=6-9 mice per group). (C-D) Immunostaining for VEGFα and αSMA shows increased VEGFα

expression in *Foxf1*$^{WT/S52F}$ lungs. Five random images per mouse were used to quantify the data (n=4 mice per group). Scale bars are 20μm. (E-F) Immunostaining for HIF-1α and αSMA shows that there is no significant difference in HIF-1α staining between *Foxf1*$^{WT/S52F}$ and *WT* lungs (n=4 mice per group). Scale bars are 20μm. (G-H) Expression levels of VEGFα and HIF-1α are similar in pulmonary artery walls of *Foxf1*$^{WT/S52F}$ and *WT* mice. Five random lung images per mouse were used to quantify the data (n=4 mice per group). NS indicates no significant difference, * indicates $p < 0.05$.

Supplemental Figure VI. Histological evaluation of *Foxf1*$^{WT/S52F}$ embryos shows a lack of cardiac hypertrophy at E17.5. H&E staining of E17.5 embryos shows thoracic cavity (A) and the heart (B) of *WT* and *Foxf1*$^{WT/S52F}$ embryos. *Foxf1*$^{WT/S52F}$ hearts exhibit normal structure of RV and LV. Scale bars: A, 2mm; B, 0.4mm. Abbreviations: Lu, lung; Th, thymus; RV, right ventricle; LV, left ventricle.

Supplemental Figure VII. *Foxf1*$^{WT/S52F}$ mice exhibit increased mortality and decreased body weight in the first 4 weeks after birth. (A) Table shows body weights and the number of alive *WT* and *Foxf1*$^{WT/S52F}$ mice during the first 4 weeks after birth. (B) Body weights of *WT* and *Foxf1*$^{WT/S52F}$ mice are compared between P0 to P28 (n=6-32 mice per group). Dotted line shows 6g of body weight, which was used to sub-divide *Foxf1*$^{WT/S52F}$ P28 mice into 2 groups: *L-Foxf1*$^{WT/S52F}$ *and H-Foxf1*$^{WT/S52F}$. (C) Photograph shows body sizes of an alive *WT* mouse and dead *Foxf1*$^{WT/S52F}$ littermate at P8. Scale bars are 10mm. (D) H&E staining of heart transverse sections shows RV hypertrophy in dead *Foxf1*$^{WT/S52F}$ P8 mouse. Scale bars are 0.8mm. NS indicates no significant difference, **** indicates $p < 0.0001$. Abbreviation: RV, right ventricle; P8, postnatal day 8.

Supplemental Figure VIII. Measurements of body weights and heart weights of *WT* and *Foxf1*$^{WT/S52F}$ mice at P28. (A) Photograph shows the size of *WT* P28 mouse compared to *Foxf1*$^{WT/S52F}$ littermates with high (*H-Foxf1*$^{WT/S52F}$) and low body weight (*L-Foxf1*$^{WT/S52}$). (B)

Photograph shows hearts of *WT*, *L-Foxf1*$^{WT/S52F}$ and *H-Foxf1*$^{WT/S52F}$ littermates at P28. (C) Heart weights of *L-Foxf1*$^{WT/S52F}$ mice are lower than *WT* and *H-Foxf1*$^{WT/S52F}$ littermates (n=6-10 mice per group). (D) The ratio of heart weight to body weight is higher in *L-Foxf1*$^{WT/S52F}$ mice compared to *WT* and *H-Foxf1*$^{WT/S52F}$ littermates (n=6-10 mice per group). NS indicates no significant difference, ** indicates $p < 0.01$, **** indicates $p < 0.0001$.

Supplemental Figure IX. *Foxf1*$^{WT/S52F}$ mice exhibit increased expression of genes associated with cardiac hypertrophy. qRT-PCR shows increased *Nppa* (A)*, Nppb* (B) and *Myh7* mRNAs (C), the *Myh7*/*Myh6* ratio (E), and *H19* lnRNA (F) in *L-Foxf1*$^{WT/S52F}$ hearts at P28. There is no significant difference in *Myh6* mRNA in *WT*, *H-Foxf1*$^{WT/S52F}$ and *L-Foxf1*$^{WT/S52F}$ hearts (D). mRNAs were normalized using *β-actin* mRNA (n=5-11 mice per group). NS indicates no significant difference, * indicates $p < 0.05$, ** indicates $p < 0.01$, **** indicates $p < 0.0001$.

Supplemental Figure X. Lack of cardiac fibrosis in *Foxf1*$^{WT/S52F}$ mice. (A-B) Immunostaining for Endomucin (green) shows no significant difference in capillary density in the right ventricles (RV) of *WT*, *H-Foxf1*$^{WT/S52F}$ and *L-Foxf1*$^{WT/S52F}$ mice at P28. Heart sections were counterstained with DAPI (blue). Five random heart images per mouse (n=5-6 mice per group) were used for quantification. Scale bars are 100μm. (C) Sirius red staining of heart sections shows no visual difference in collagen deposition between *WT*, *H-Foxf1*$^{WT/S52F}$ and *L-Foxf1*$^{WT/S52F}$ hearts at P28. Bottom panels show RV myocardium. Scale bars are 0.8mm (top panels) and 200μm (bottom panels). (D-E) WGA staining show similarities in the size of left ventricular (LV) cardiomyocytes in *WT*, *H-Foxf1*$^{WT/S52F}$ and *L-Foxf1*$^{WT/S52F}$ hearts at P28. Average cell sizes were determined using 5 random heart images per mouse (n=7-8 mice per group). Scale bars are 100μm. NS indicates no significant difference.

Supplemental Figure XI. *L-Foxf1*$^{WT/S52F}$ lungs exhibit increased expression of hypoxia-associated genes. (A) qRT-PCR shows no significant differences in *Hif1a* mRNA in *WT*, *H-*

Foxf1$^{WT/S52F}$ and *L-Foxf1*$^{WT/S52F}$ lungs at P28. mRNAs were normalized using β-*actin* mRNA (n=7-9 mice per group). (B-F) qRT-PCR shows increased *Vegfa*, *Binp3*, *Epas1* and *Slc2a1* mRNAs, and *H19* lnRNA in lungs of *L-Foxf1*$^{WT/S52F}$ mice (n=5-9 mice per group). NS indicates no significant difference, ** indicates $p < 0.01$, *** indicates $p < 0.001$, **** indicates $p < 0.0001$.

Supplemental Figure XII. HIF-1α staining is not altered in *Foxf1*$^{WT/S52F}$ lungs. Immunostaining for HIF-1α and αSMA (A) shows no significant difference in the number of HIF-1α-positive cells (B) and the number of cells with nuclear HIF-1α staining (C) between *WT*, *H-Foxf1*$^{WT/S52F}$ and *L-Foxf1*$^{WT/S52F}$ lungs at P28. Inserts show high magnification images of cells with HIF-1α staining. Five random images per mouse (n=3 mice per group) were used for quantification. Scale bars are 50μm. NS indicates no significant difference.

Supplemental Figure XIII. *Foxf1*$^{WT/S52F}$ mice exhibit decreased proliferation of pulmonary endothelial cells at P7. FACS analysis was performed using enzymatically digested lung tissue of P7 mice. Proliferation of endothelial cells ($CD31^+CD45^-Ki\text{-}67^+$) was lower in the lungs of *Foxf1*$^{WT/S52F}$ mice compared to *WT* lungs (n=5-6 mice per group). Cell were fixed and permeabilized prior to intracellular Ki-67 staining. The gating for Ki-67 staining was determined using isotype control antibodies. * indicates $p < 0.05$.

Supplemental Figure XIV. Juvenile *L-Foxf1*$^{WT/S52F}$ mice exhibit remodeling of pulmonary arteries. (A-C) Measurements of arterial wall thickness show thickening of small (inner diameter < 20μm), medium (inner diameter = 20-50μm) and large (inner diameter > 50μm) pulmonary arteries in *L-Foxf1*$^{WT/S52F}$ mice at P28. Five random lung images per mouse were used to quantify the data (n=5 mice per group). (D) Table shows the percentage of partially remodeled pulmonary arteries in *WT*, *H-Foxf1*$^{WT/S52F}$ and *L-Foxf1*$^{WT/S52F}$ mice at P28. NS indicates no significant difference, * indicates $p < 0.05$, *** indicates $p < 0.001$, **** indicates $p < 0.0001$.

Supplemental Figure XV. *Foxf1*$^{WT/S52F}$ mice exhibit increased proliferation of pulmonary αSMA^{+} cells at P7. (A-C) Immunostaining of lung sections was performed using Ki-67, αSMA, and PDGFRα antibodies to identify fibroblasts and smooth muscle cells (arrows). Right and middle panels show the area in the yellow box. Percentages of Ki-67^{+}αSMA^{+} myofibroblasts and arterial smooth muscle cells were increased in *L-Foxf1*$^{WT/S52F}$ mice at P7. Ki-67^{+} cells were counted using 5 random lung images per mouse (n=7-8 mice per group). Scale bars are 50μm. (D-E) Immunostaining shows no difference in the number of Ki-67^{+}PECAM1^{+} endothelial cells lining pulmonary arteries in *L-Foxf1*$^{WT/S52F}$ and *WT* mice (n=4 mice per group). NS indicates no significant difference, **** indicates $p < 0.0001$.

Supplemental Figure XVI. FOXF1 is not expressed in vascular smooth muscle cells. Immunostaining of lung sections from P7 (A) and P28 *WT* mice (B) shows that FOXF1 does not colocalize with αSMA in vascular smooth muscle cells. FOXF1 is expressed in a subset of arterial endothelial cells and parenchymal cells. Sections were counterstained with DAPI. Scale bars are 50μm.

Supplemental Figure XVII. Human ACDMPV lungs exhibit increased fibrotic deposition. Sirius red staining shows increased collagen deposition in alveolar and perivascular regions of human ACDMPV lungs (n=3). An age-matched donor human lung is used as a control. Scale bar is 300μm.

Supplemental Figure XVIII. Increased expression of profibrotic genes in human ACDMPV lungs. Microarray analysis of whole lung RNAs shows increased expression of profibrotic genes and *H19* lncRNA in ACDMPV lungs (n=8) compared to age-matched donor human lungs (n=5). * indicates $p < 0.05$, ** indicates $p < 0.01$.

Supplemental Figure XIX. *Foxf1*$^{WT/S52F}$ lungs exhibit an increased percentage of pulmonary CD140a$^{+}\alpha$SMA^{+} myofibroblasts at P7. FACS analysis was performed using enzymatically digested lung tissue of P7 mice. Percentage of CD140a$^{+}\alpha$SMA^{+} myofibroblasts (CD140a$^{+}\alpha$SMA^{+}CD31^{-}CD45^{-}) was higher among CD140a^{+} fibroblasts (CD140a^{+}CD31^{-}CD45^{-}) in *Foxf1*$^{WT/S52F}$ lungs compared to lungs of *WT* littermates (n=3-4 mice per group). Cell were fixed and permeabilized to detect intracellular αSMA. The gating of CD140a (PDGFRα) and αSMA staining was determined using isotype control antibodies. * indicates $p < 0.05$.

Supplemental Figure XX. ESC-derived cells are present in lung tissue of chimeric mice. (A) Images show cell colonies of *tdT-S52F Foxf1* ESCs (red) and *GFP-WT* ESCs (green). (B) Confocal images of frozen sections from P7 chimeric lungs show contribution of *tdT-S52F Foxf1* ESCs and *GFP-WT* ESCs to the same lungs. Scale bars: A, 10μm; B, 100μm. Abbreviations: V, vessel; Br, bronchiole.

Supplemental Figure XXI. FACS analysis shows similar contribution of *tdT-S52F Foxf1* ESCs and *GFP-WT* ESCs to pulmonary pericytes, endothelial, epithelial, and hematopoietic cells. FACS analysis of enzymatically-digested lung tissue from P7 chimeric mice was performed to identify the contribution of donor *tdT-S52F Foxf1* ESCs and *GFP-WT* ESCs to CD31^{+}CD45^{-} endothelial cells (A), CD326^{+}CD31^{-}CD45^{-} epithelial cells (B), NG2^{+}CD31^{-}CD45^{-}CD326^{-}CD140a^{-} pericytes (C), and CD45^{+}CD31^{-} hematopoietic cells (D) (n=6 mice per group). Cells that are negative for both *GFP* and *tdTomato* originated from endogenous (not labeled) ESCs, whereas GFP^{+}tdTomato^{+} cells formed by a fusion of donor-derived cells. NS indicates no significant difference, * indicates $p < 0.05$, ** indicates $p < 0.01$, *** indicates $p < 0.001$, **** indicates $p < 0.0001$.

Supplemental Figure XXII. Nanoparticle delivery of *Stat3* cDNA increases capillary density in the lungs of *Foxf1*$^{WT/S52F}$ mice. (A) Immunostaining for Endomucin and p-STAT3^{+}

shows the alveolar capillary network in mice treated with nanoparticles containing either a *CMV-Stat3* or a *CMV-empty* vector. Inserts show high magnification images of p-STAT3^{+} endothelial cells. Scale bars are 100μm. (B-C) Endomucin and p-STAT3 stained images were quantitated for capillary density and the number of endothelial cells expressing p-STAT3. Five random microscope images were used per mouse (n=4-5 mice per group). (D-E) qRT-PCR shows increased *Pecam1* and *Flk1* mRNAs in lungs from *Foxf1*$^{WT/S52F}$ mice treated with *CMV-Stat3* (STAT3) compared to *Foxf1*$^{WT/S52F}$ mice treated with *CMV-empty* (Emp). mRNAs were normalized using *β-actin* mRNA (n=5-7 mice per group). NS indicates no significant difference, * indicates $p < 0.05$, ** indicates $p < 0.01$.

Supplemental Figure XXIII. Nanoparticle delivery of *Stat3* cDNA increases STAT3 staining in alveoli but does not change STAT3 in arterial smooth muscle cells. Immunostaining for αSMA and STAT3^{+} shows increased STAT3 in alveolar region of *Foxf1*$^{WT/S52F}$ mice treated with *CMV-Stat3* nanoparticles (STAT3) compared to a *CMV-empty* control (A-B). There are no significant differences in STAT3 staining in pulmonary artery smooth muscle cells between all groups of mice (C). The number of STAT3^{+}αSMA^{+} cells were counted using 5 random lung images per mouse (n=4 mice per group). Scale bars are 50μm. NS indicates no significant difference, * indicates $p < 0.05$.

Supplemental Figure XXIV. Nanoparticle delivery of *Stat3* cDNA does not affect p-STAT3 in pulmonary artery smooth muscle cells. Immunostaining for αSMA and p-STAT3^{+} shows no significant difference in p-STAT3 in pulmonary artery smooth muscle cells of *WT* and *Foxf1*$^{WT/S52F}$ mice treated with nanoparticles containing either a *CMV-Stat3* of a *CMV-empty* vector. The number of p-STAT3^{+}αSMA $^{+}$ cells were counted using 5 random lung images per mouse (n=4 mice per group). Scale bars are 50μm. NS indicates no significant difference.

Supplemental Figure XXV. Nanoparticle delivery of *Stat3* cDNA improves heart function in *Foxf1*$^{WT/S52F}$ mice. (A) Echocardiography shows an improved pulmonary artery velocity curve in *Foxf1*$^{WT/S52F}$ mice injected with STAT3 nanoparticles compared to *CMV-empty* controls. Nanoparticles were injected at P2. Echocardiography was performed at 4 months of age. (B-D) Nanoparticle delivery of *Stat3* cDNA increases stroke volume (SV), S wave and cardiac output (CO) in *Foxf1*$^{WT/S52F}$ mice (n=4-5 mice per group). NS indicates no significant difference, * indicates $p < 0.05$, ** indicates $p < 0.01$.

Supplemental Figure XXVI. Nanoparticle treatment with *Stat3* cDNA decreases the size of RV cardiomyocytes in *Foxf1*$^{WT/S52F}$ mice. (A) Wheat germ agglutinin (WGA) staining shows that nanoparticle delivery of a *CMV-Stat3* vector (STAT3) decreases the size of cardiomyocytes in the right ventricle of *Foxf1*$^{WT/S52F}$ *mice* compared to *Foxf1*$^{WT/S52F}$ mice treated with nanoparticles containing a *CMV-empty* vector (Emp). Nanoparticles were injected at P2. Mice were harvested at P28. (B) WGA-stained images were quantitated using 5 random microscope images per mouse (n=4-5 mice per group). Scale bars are 100μm. NS indicates no significant difference, * indicates $p < 0.05$.

Supplemental Figure XXVII. Nanoparticle treatment with *Stat3* cDNA does not affect capillary density in the right ventricle of *Foxf1*$^{WT/S52F}$ mice. (A-B) Immunostaining for Endomucin (green) shows that the capillary density in the right ventricles of *Foxf1*$^{WT/S52F}$ and *WT* mice is similar after nanoparticle treatment with CMV-*Stat3* (STAT3) or *CMV-empty* (Emp). Nanoparticles were injected at P2. Mice were harvested at P28. Slides were counterstained with DAPI (blue). Endomucin-stained images were quantitated using 5 random microscope images per mouse (n=4 mice per group). Scale bars are 100μm. (C-D) FACS analysis of enzymatically-digested *WT* lung, heart, liver, kidney and spleen tissues shows no significant difference in the percentage of endothelial cells ($CD31^{+}CD45^{-}$) targeted by the nanoparticles (n=4 mice per group). Nanoparticles were labeled by the DyLight 650 quantum dots and

contained *CMV-empty* vector. Organs were harvested 48 hrs after i.v. injection of the nanoparticles. NS indicates no significant difference.

Supplemental Figure XXVIII. Nanoparticle treatment with *Stat3* cDNA does not affect p-STAT3 in heart and liver. Immunostaining for Endomucin and p-STAT3^{+} (A) shows no significant difference in the numbers of p-STAT3^{+} endothelial cells in hearts (B) and livers (C) of *WT* and *Foxf1*$^{WT/S52F}$ mice treated with nanoparticles containing either a *CMV-Stat3* of a *CMV-empty* vector. The number of p-STAT3^{+}Endomucin^{+} cells were counted using 5 random lung images per mouse (n=3-4 mice per group). Scale bars are 100μm. NS indicates no significant difference.

Supplemental Figure XXIX. Nanoparticle treatment with *Stat3* cDNA decreases alveolar simplification in *Foxf1*$^{WT/S52F}$ lungs. (A) H&E staining of lung sections shows nanoparticle delivery of *Stat3* cDNA (STAT3) reduces the alveolar simplification in *Foxf1*$^{WT/S52F}$ mice compared to *Foxf1*$^{WT/S52F}$ mice treated with nanoparticles containing an empty vector (Emp). Nanoparticles were injected at P2. Mice were harvested at P28. Scale bars are 50μm. (B) Mean linear intercept (MLI) was determined using 5 random H&E-stained images from each of 3 lung sections per mouse (n=5-6 mice per group). NS indicates no significant difference, * indicates $p < 0.05$.

Supplemental Figure XXX. Nanoparticle delivery of *Stat3* cDNA reduces small artery remodeling in *Foxf1*$^{WT/S52F}$ lungs. (A-B) Immunostaining shows that nanoparticle delivery of *Stat3* cDNA (STAT3) decreases αSMA staining (red) in *Foxf1*$^{WT/S52F}$ mice compared to *Foxf1*$^{WT/S52F}$ mice treated with nanoparticles containing a *CMV-empty* vector (Emp). Nanoparticles were injected at P2. Mice were harvested at P28. Slides were counterstained with DAPI (blue). αSMA-stained images were quantitated using 5 random microscope images per mouse (n=6-8 mice per group). Scale bars are 150μm. (C) qRT-PCR shows decreased

Acta2 mRNA in lungs of *Foxf1*$^{WT/S52F}$ mice treated with *CMV-Stat3* compared to *Foxf1*$^{WT/S52F}$ mice treated with nanoparticles containing an empty vector. *Acta2* mRNA was normalized using *β-actin* mRNA (n=6-7 mice per group). NS indicates no significant difference, * indicates $p < 0.05$, ** indicates $p < 0.01$, *** indicates $p < 0.001$, **** indicates $p < 0.0001$.

Supplemental Figure XXXI. Nanoparticle delivery of *Stat3* cDNA does not affect expression of epithelial markers in the lung. Immunostaining for T1α (red) and pro-SPC (green) shows that nanoparticle delivery of *Stat3* cDNA does not change the expression of T1α and pro-SPC in *Foxf1*$^{WT/S52F}$ and *WT* mice. Nanoparticles were injected at P2. Mice were harvested at P28. DAPI (blue) was used to stain cell nuclei. Scale bars are 100μm.

Supplemental Figure XXXII. Nanoparticle treatment with *Stat3* cDNA decreases fibrotic lung remodeling in *Foxf1*$^{WT/S52F}$ mice. (A-B) Sirius red staining shows decreased collagen deposition in alveolar regions of *Foxf1*$^{WT/S52F}$ mice treated with *CMV-Stat3* nanoparticles (STAT3) compared to *Foxf1*$^{WT/S52F}$ mice treated with nanoparticles containing an empty vector (Emp). Nanoparticles were injected at P2. Mice were harvested at P28. Collagen staining was quantitated using 5 random microscope images per mouse (n=6-7 mice per group). Scale bars are 50μm. (C) qRT-PCR shows that nanoparticle delivery of *Stat3* cDNA decreases mRNAs of *Col1a1*, *Col3a1* and *Vimentin* in *Foxf1*$^{WT/S52F}$ lungs (n=5-7 mice per group). mRNAs were normalized using *β-actin* mRNA. NS indicates no significant difference, ** indicates $p < 0.01$, **** indicates $p < 0.0001$.

Supplemental Figure XXXIII. Nanoparticle delivery of *Stat3* cDNA reduces *Vegfa* mRNA in *Foxf1*$^{WT/S52F}$ lungs. qRT-PCR shows that nanoparticle delivery of *Stat3* cDNA does not affect *Hif1a* mRNA (A) but decreases *Vegfa* mRNA (B) in *Foxf1*$^{WT/S52F}$ lungs (n=6-7 mice per group). mRNAs were normalized using *β-actin* mRNA. Nanoparticles were injected at P2. Mice were harvested at P28. NS indicates no significant difference, ** indicates $p < 0.01$.

Supplemental Figure XXXIV. Nanoparticle delivery of *Stat3* cDNA increases body weight of *Foxf1*$^{WT/S52F}$ mice at P28. Body weights of *Foxf1*$^{WT/S52F}$ mice treated with *CMV-Stat3* nanoparticles (STAT3) are higher compared to *L-Foxf1*$^{WT/S52F}$ mice treated with nanoparticles containing an empty vector (Emp) (n=6-15 mice per group). Nanoparticles were injected at P2. Body weights were measured at P28. NS indicates no significant difference, * indicates $p < 0.05$, **** indicates $p < 0.0001$.

Supplemental Figure XXXV. Nanoparticle delivery of *Stat3* cDNA reduces mortality of *Foxf1*$^{WT/S52F}$ mice. (A) Lung weights are increased in *Foxf1*$^{WT/S52F}$ mice treated with *CMV-Stat3* nanoparticles (STAT3) compared to *Foxf1*$^{WT/S52F}$ mice treated with nanoparticles containing an empty vector (Emp) (n=4-5 mice per group). Nanoparticles were injected at P2. Mice were harvested at P28. (B) Table shows the 4-week mortality in *Foxf1*$^{WT/S52F}$ and *WT* mice injected at P2 with nanoparticles containing *CMV-Stat3* cDNA or an empty vector. Untreated *Foxf1*$^{WT/S52F}$ mice (n=366) were used as an additional control group to show mortality rates in *Foxf1* mutant mice without nanoparticle treatment. NS indicates no significance, * indicates $p < 0.05$, ** indicates $p < 0.01$.